HIAS-E-142

# Testing and Quantifying Economic Resilience

Naoko Hara [(a)], Yohei Yamamoto [(b)]

*(a) Seikei University*
*(b) Hitotsubashi University*

November 8, 2024

Hitotsubashi Institute for Advanced Study, Hitotsubashi University
2-1, Naka, Kunitachi, Tokyo 186-8601, Japan
tel:+81 42 580 8668 http://hias.hit-u.ac.jp/

HIAS discussion papers can be downloaded without charge from:
https://hdl.handle.net/10086/27202
https://ideas.repec.org/s/hit/hiasdp.html

# Testing and Quantifying Economic Resilience

Naoko Hara* Yohei Yamamoto†

Seikei University Hitotsubashi University

November 8, 2024

**Abstract**

We propose a formal testing procedure to examine resilience of an economy. Our approach is applicable even when a cross-section of control group is unavailable and circumvents potential bias in time-series regressions using data that includes structural breaks. We provide measures of shock absorption and cumulative recovery. Our empirical analysis reveals that most of the advanced countries were not resilient to the Global Financial Crisis, while many were so during the COVID-19 pandemic. Potential determinants of economic resilience such as financial leverage and labor market regulation may have negative correlations with these measures and other determinants have heterogenous associations depending on the nature of the crisis.

**JEL Classification Numbers:** C12, C53, E57

**Keywords:** Economic Resilience; Counterfactual Forecast; Pretesting; Global Financial Crisis; COVID-19 Pandemic

*Seikei University, Faculty of Economics, 3-3-1 Kichijoji-Kitamachi, Musashino, Tokyo, Japan 180-8633 (naoko-hara@econ.seikei.ac.jp).

†Hitotsubashi University, Department of Economics, 2-1 Naka, Kunitachi, Tokyo, Japan 186-8601 (yohei.yamamoto@r.hit-u.ac.jp).

## 1 Introduction

The global economy experiences a business cycle marked by a sharp drop and protracted recovery.[1] Recent Global Financial Crisis (GFC) and the COVID-19 pandemic, have accentuated this feature, prompting academia and policy makers to address the question of whether post-crisis economic growth path has returned to the pre-crisis growth trajectory. This is tied to the traditional concept of economic hysteresis (Blanchard and Summers, 1987; Cerra and Saxena, 2008; Reinhart and Rogoff, 2014, Ball, 2014; Cerra et al., 2023) and an increasingly popular notion of economic resilience (Briguglio et al., 2009, Fingleton et al., 2012, Martin, 2012, Jollès et al., 2023).[2] Some studies have applied existing econometric methods and others tailored new ones to tackle this question. For example, Cerra and Saxena (2008) and Fingleton et al. (2012) conducted impulse response analyses to a crisis shock using full sample panel data, namely, the period including the crisis event. Aikman et al. (2022) proposed a test to compare the mean of multi-year growth rates after the crisis with those in other periods. Blanchard et al. (2015) produced a forecast based on a linear trend model with an interval that accounts for uncertainty associated with the trend slope. The effect of crisis shock is also tested in the literature of causal inference. A leading example is the synthetic control method (SCM) of Abadie et al. (2010) aiming to forecast a counterfactual output by using control sample that had no effects. Cavallo et al. (2013) examined the impact of natural disasters on GDP by using control countries that had no disasters. However, such a control sample is often unavailable when the crisis spreads worldwide.

In this study, we propose a formal testing procedure based on a time-series forecast to assess whether the actual post-crisis output has returned to the counterfactual trajectory of no crisis. We focus on a linear trend with persistent noise model as it is a simple yet widely accepted model to capture the dynamics of log real GDP (Nelson and Plosser, 1982; Campbell and Mankiw, 1987; Perron, 1989; Stock, 1991). We incorporate uncertainty associated with future disturbances, parameter estimation, and their interactions, while the well-known dichotomy of trend-stationary and random walk models is addressed by unit root pretesting. We confirm that this method achieves a good finite sample coverage even when the persistence

[1] In empirical business cycle studies, this pattern may have been understood as asymmetricity (Neftci, 1984, Hamilton, 1989, Acemoglu et al., 1997, Clements and Krolzig, 2003, Morley and Piger, 2012) or negative skewness (De Long and Summers, 1984; Bai and Ng, 2005; Plagborg-Møller et al., 2020; Jensen et al. 2020; Iseringhausen et al., 2023).

[2] In the existing literature, economic resilience is defined as the capacity of an economy to recover quickly from the effect of shock (Noy and Yonson, 2018, Diop et al., 2021). The concept of resilience itself has been popular and is increasingly so in many fields of natural and social sciences such as engineering, psychology.

parameter is close to one and the interval length equal to the model with good coverage.

This seemingly straightforward approach will shed a new light on the methodological aspect of the aforementioned literature. First, our approach leaves the actual growth path after the crisis completely unrestricted thus no model needs to be estimated using the post-crisis data, circumventing estimation bias due to the data contaminated by the crisis. Second, it is capable of conducting real-time inference as new data arrives. Third, it dispenses with a cross-section of control countries that experienced no crisis impacts, ensuring applicability to global crises. Fourth, it delivers a unit free measure of recovery patterns among countries which might have had heterogenous effects. Specifically, we propose a measure of shock absorption defined by the bottom of standardized statistics and a measure of recovery as the ratio of the actual cumulative recovery to the counterfactual cumulative loss from no recovery. These tools offer a multifaceted outcome to evaluate economic resilience.

Our empirical analysis using the log real GDP of 18 advanced OECD countries reveals that most countries were not resilient to the GFC shock and potential hysteresis effects are suggested. The recovery patterns are represented by L-shapes. However, during the COVID-19 pandemic, the deep troughs were followed by fast recoveries to the counterfactual pre-crisis growth path and they exhibited V-shape patterns. We also illustrate bivariate associations of these measures with potential determinants of economic resilience suggested by the literature. We show that determinants such as financial leverage and labor market regulation have negative correlations with shock absorption and cumulative recovery measures, while correlations of government debt ratio with these measures are opposite across the two crises. Furthermore, R&D spending, trade openness, and inequality have heterogenous relationships with recovery measure across the two crises. Overall, some determinants may have negative correlations with shock absorption and recovery across the two crises; however, other factors vary in their associations, depending on the nature of the crisis.

The rest of this study is organized as follows. Section 2 explains the model and the hypotheses. We also elaborate on the motivations and advantages of our approach compared to the existing methods. In Section 3, we establish forecasting error variances for both the trend-stationary and random walk models and describe a simple pretesting method. We also provide quantitative measures of shock absorption and cumulative recovery. Section 4 conducts a Monte Carlo simulation to assess finite sample properties of the forecasting intervals. In Section 5, we present empirical analysis using the log real GDP of 18 advanced OECD countries. Section 6 provides some concluding remarks.

## 2 Motivation

Let $y_t$ be a time-series data such as economic output or employment at period $t$. The data is available for $t = 1, ..., T + H$ where $t = T + H$ is the present period, while the crisis occurred at a known date $t = T$. We call the sample for $t \in [1, T]$ the pre-crisis period and that for $t \in [T+1, T+H]$ the post-crisis period. The goal of this study is to assess whether the post-crisis output $y_{T+h}$ has recovered the counterfactual growth path as if no crisis had occurred. To this end, we follow the convention such as Nelson and Plosser (1982) and assume that $y_t$ follows the linear trend and persistent noise model if no crisis had occurred.

$$y_t = \mu + \beta t + u_t, \tag{1}$$

$$u_t = \rho u_{t-1} + \varepsilon_t, \tag{2}$$

where $\varepsilon_t$ is the disturbance term assumed to follow $i.i.d.N(0, \sigma^2)$ for $t = 1, \cdots, T$. The coefficients $\mu$ and $\beta$ in (1) are unknown fixed parameters for the intercept and the slope of linear trend, respectively. The unknown persistence parameter $\rho$ in (2) is assumed to lie in the interval $(-1, 1]$. We assume $u_0 \sim N(0, \sigma^2/(1-\rho^2))$ when $|\rho| < 1$ and $u_0 = 0$ when $\rho = 1$.

There are several potential approaches to achieve our research goal. The first approach investigates whether $y_t$ has a stochastic trend by using time-series data for $t = 1, ..., T + H$. If the null hypothesis of $\rho = 1$ is not rejected, $y_t$ is considered to have a stochastic trend, indicating that shocks may have permanent effects. This provides indirect evidence of non-resilient economy as the crisis could permanently decrease the level of $y_t$. If $\rho = 1$ is rejected in favor of $|\rho| < 1$, $y_t$ is considered trend stationary and any shocks have merely transitory effects, suggesting that the economy is resilient. However, such unit root tests for $\rho = 1$ notoriously have low power when the data has a structural break as it can significantly bias the persistence parameter estimate upwardly (Perron, 1989). This is likely if the entire sample period is used. Instead, if the test is implemented using the pre-crisis sample only, out-of-sample validity must be ensured. The same caveat applies to impulse response analyses conducted by many studies (Cerra and Saxena, 2008, Fingleton et al., 2012), since estimates of the persistence parameters using data with a break may have an upward bias.

Another time-series approach is to assess whether the model had a structural change at the crisis and to separately estimate models for the pre- and the post- crisis periods. Figure 1 illustrates potential patterns of the post-crisis growth path.[3] In Cases A, B and C, the

[3] See Martin (2012) and Fingleton et al. (2012) for similar presentation. Fingleton et al. (2012) introduced "engineering resilience" and "ecological resilience". The former means that the level catches up the original

intercept $\mu$ decreased, which resulted in a decline of $y_t$ at the crisis. However, the trend slope $\beta$ may have either increased (Case A), decreased (Case B) or unchanged (Case C). Case A is considered resilient while Cases B and C are non-resilient. In Case D, the trend slope decreased and the intercept changed in a specific manner so that is no abrupt level shift occurred. This pattern may also be considered non-resilient. Therefore, one may assess economic resilience by estimating the trend slope and the intercept before and after the crisis, respectively. However, data is typically scarce for the post-crisis period and a certain time must have elapsed to assess economic resilience. Also, the model specification after the crisis is highly uncertain and the linear model may not be relevant after the crisis.

When a panel data set which includes countries which had a crisis effect (treated group) and those which had no crisis effect but have the same trend (control group) is available, a more recent literature on causal inference offers an additional perspective. For example, the synthetic control method (SCM) proposed by Abadie and Gardeazabal (2003) and Abadie et al. (2010) produces a counterfactual forecast of no crisis for the treated country, given a sample of control group is available. The SCM uses a cross-section information of the control group for the post-crisis period to produce a counterfactual forecast for the treated units. It can avoid time-series modeling and estimation of the persistence parameters. For example, Cavallo et al. (2013) examined the impact of natural disasters on GDP by using a group of countries that had the same secular trends but no disasters. However, this method is subject to some delay in obtaining data for all control countries. More importantly, it is not applicable when the crisis had worldwide effects, because no control countries are available.

The approach this study proposes uses a time-series technique to produce a counterfactual forecast for the post-crisis output growth trajectory as if no crisis had occurred. Then, at each horizon $h$, it assesses whether the actual output is included in the counterfactual forecasting interval. Importantly, our approach leaves the actual growth path after the crisis completely unrestricted and no model needs to be specified for the typically short post-crisis sample period. In addition, it is capable of conducting inference as new data arrives, promptly judging economic resilience. We discuss some econometric issues in constructing the counterfactual forecast interval from (1) and (2) in the next section.

trajectory, while the latter allows level shifts to a new stable equilibrium. We do not rely on explicit modelling after the crisis and such concepts are not discussed in this study, although they can be assessed by inspecting the recovery pattern as we do in Section 6.

## 3 Forecasting methods

### 3.1 Trend-stationary model

We first consider forecasting interval produced by models (1) and (2) when $|\rho| < 1$ is assumed. The model can be efficiently estimated by a feasible generalized least squares (FGLS) or the maximum likelihood method. We follow Ng and Vogelsang (2002) and Falks and Roy (2005) and use the Prais-Winsten FGLS (Prais and Winsten, 1954). Let the vector form of (1) be

$$y_t = z_t'\delta + u_t,$$

where $z_t \equiv [1, t]'$ and $\delta \equiv [\mu, \beta]'$. If we denote the regressor matrix by $Z = [z_1', ..., z_T']'$, the Prais-Winsten FGLS estimator is

$$\hat{\delta} = (Z'\hat{\Omega}^{-1}Z)^{-1}(Z'\hat{\Omega}^{-1}y),$$

where

$$\hat{\Omega}^{-1} = \begin{bmatrix} 1 & -\hat{\rho} & & 0 & 0 \\ -\hat{\rho} & 1+\hat{\rho}^2 & & 0 & 0 \\ 0 & -\hat{\rho} & \ddots & -\hat{\rho} & 0 \\ 0 & 0 & & 1+\hat{\rho}^2 & -\hat{\rho} \\ 0 & 0 & & -\hat{\rho} & 1 \end{bmatrix},$$

while $\rho$ is estimated as the first order sample autocorrelations of $\hat{u}_t = y_t - z_t'\hat{\delta}^{(0)}$ for $t = 1, ..., T$, where $\hat{\delta}^{(0)}$ is an initial estimate by ordinary least squares (OLS). The procedure may be iterated after we obtain $\hat{\delta}$ until it converges.

Once $\delta$ and $\rho$ are estimated, the $h$ period ahead forecast is constructed by the so-called best linear unbiased prediction proposed by Goldberger (1962)[4]:

$$\hat{y}_{T+h|T} = z_{T+h}'\hat{\delta} + \hat{\rho}^h(y_T - z_{T+h}'\hat{\delta}).$$

[4] An alternative forecasting method of the trend-stationary model is to use a reparametrized version of models (1) and (2), the so-called Durbin's regression

$$y_t = \mu^* + \beta^* t + \rho y_{t-1} + \varepsilon_t,$$

where $\mu^* = \mu(1-\rho) + \beta\rho$ and $\beta^* = \beta(1-\rho)$. Ng and Vogelsang (2002) and Falk and Roy (2005) compared finite sample mean squared errors of these forecasts and concluded that the Prais-Winsten FGLS gives the best performance. In Appendix B, we compare the coverage rate and the average length of forecast intervals of these methods.

The forecasting error $\hat{\varepsilon}_{T+h|T} = y_{T+h} - \hat{y}_{T+h|T}$ becomes

$$\begin{aligned} y_{T+h} - \hat{y}_{T+h|T} &= z'_{T+h}\delta + u_{T+h} - z'_{T+h}\hat{\delta} - \hat{\rho}^h(y_T - z'_T\hat{\delta}), \\ &= \textstyle\sum_{l=0}^{h-1} \rho^l \varepsilon_{T+h-l} + (z'_{T+h} - \rho^h z_T)(\delta - \hat{\delta}) \\ &\quad +(\rho^h - \hat{\rho}^h)u_T + (\rho^h - \hat{\rho}^h)z_T(\delta - \hat{\delta}). \end{aligned} \tag{3}$$

The first term of (3) captures intrinsic future disturbances $\varepsilon_{T+h-l}$ for $l = 1, ..., h-1$ whose effect is unavoidable in any forecasting exercises. The second to the fourth terms pertain to effects of parameter estimation errors which diminish as $T \to \infty$. More precisely, the second term comes from the estimate $\hat{\delta}$ and the third term pertains to $\hat{\rho}$. The fourth term appears as an interaction between them. The effect of parameter estimation on the variance has been discussed at length by, for example, Sampson (1991) and Clements and Hendry (2001).

Based on this expression, the following result for the asymptotic forecasting variance is obtained. Note that if an estimator $\hat{\delta}$ has an asymptotic result $\sqrt{T}(\hat{\delta} - \delta) \xrightarrow{d} N(0, \Sigma_\delta)$ with $\Sigma_\delta$ a fixed covariance matrix as $T \to \infty$, we call $T^{-1}\Sigma_\delta$ the asymptotic variance of $\hat{\delta}$ denoted by $AVar(\hat{\delta})$ and for a simple random variable $\varepsilon$, $AVar(\varepsilon)$ coincides with $Var(\varepsilon)$.

**Theorem 1** *Suppose $y_t$ for $t = 1, ..., T+H$ is generated by (1) and (2) with $|\rho| < 1$. Let the asymptotic forecast error variance of (3) at a horizon $h = 1, ..., H$ constructed at $t = T$ be $f_{T+h|T}$. Then,*

$$f_{T+h|T} = C1_{T,h} + C2_{T,h} + C3_{T,h} + C4_{T,h}, \tag{4}$$

*uniformly in $h$ where*

$$\begin{aligned} C1_{T,h} &= \sigma^2 \textstyle\sum_{l=0}^{h-1} \rho^{2l}, \\ C2_{T,h} &= (z_{T+h} - \rho^h z_T)' AVar(\hat{\delta})(z_{T+h} - \rho^h z_T), \\ C3_{T,h} &= u_T^2 \times AVar(\hat{\rho}^h), \\ C4_{T,h} &= AVar(\hat{\rho}^h) \times z'_T AVar(\hat{\delta}) z_T. \end{aligned}$$

See Appendix A for a proof. By using an estimate for the forecast variance under Gaussian errors, the trend-stationary forecast interval can be constructed by

$$\hat{y}_{T+h|T} \pm z_{\alpha/2}\sqrt{\hat{f}_{T+h|T}}, \tag{5}$$

where $z_{\alpha/2}$ is the $100(1-\alpha/2)$ percentile of the standard normal distribution and $\hat{f}_{T+h|T}$ is an estimate of $f_{T+h|T}$. We suggest plugging $\widehat{AVar}(\hat{\delta}) = (\hat{u}'\hat{\Omega}^{-1}\hat{u}/T)(Z'\hat{\Omega}^{-1}Z)^{-1}$ into $AVar(\hat{\delta})$, $\widehat{AVar}(\hat{\rho}^h) = h^2\hat{\rho}^{2(h-1)}\widehat{AVar}(\hat{\rho})$ into $AVar(\hat{\rho}^h)$ by using the delta method, and

$\widehat{AVar}(\hat{\rho}) = (1-\hat{\rho}^2)/T$. Falk and Roy (2005) proposed a forecasting interval by using the median bias-corrected estimate for $\rho$ proposed by Roy and Fuller (2001). However, our separate investigation reveals that although the bias-corrected estimate can improve forecast interval of the trend-stationary model, it may not improve finite sample properties of the pretesting intervals. Hence, we dispense with bias-corrections in this study.

### 3.2 Random walk model

Empirical studies such as Nelson and Plosser (1982), Campbell and Mankiw (1987) and Stock (1991) provide evidence that $\rho = 1$ for the U.S. real GDP. In this subsection, we consider a random walk model in which $\rho = 1$ is imposed. This will help us reduce the number of parameters thus the estimation effect, while keeping the point forecasts unconditionally unbiased. By plugging $\rho = 1$ in (2) and combining it with (1), we get the following model

$$y_t = \beta + y_{t-1} + \varepsilon_t.$$

Furthermore, by moving $y_{t-1}$ to the left-hand-side, we obtain

$$y_t - y_{t-1} = \beta + \varepsilon_t. \tag{6}$$

This model has only one unknown coefficient $\beta$. Also, as the errors are spherical, the efficient OLS estimate for $\beta$ is simply obtained by the sample mean of the dependent variable such that $\widetilde{\beta} = \frac{1}{T-1}\sum_{t=2}^{T}(y_t - y_{t-1})$ so that $Var(\widetilde{\beta}) = \frac{\sigma^2}{T-1}$.

The $h$ period ahead forecast of $y_{T+h}$ is

$$\widetilde{y}_{T+h|T} = y_T + h\widetilde{\beta}. \tag{7}$$

When $\rho = 1$ the forecast error of the random walk model becomes

$$\begin{aligned} y_{T+h} - \widetilde{y}_{T+h|T} &= y_T + h\beta + \textstyle\sum_{l=0}^{h-1}\varepsilon_{T+h-l} - y_T - h\widetilde{\beta}, \\ &= \textstyle\sum_{l=0}^{h-1}\varepsilon_{T+h-l} + h(\beta - \widetilde{\beta}). \end{aligned} \tag{8}$$

Similar to (3), the first term pertains to the intrinsic future disturbances while the second term refers to the parameter estimation effect.

**Theorem 2** *Suppose $y_t$ for $t = 1, ..., T+H$ is generated by (1) and (2) with $\rho = 1$. Let the asymptotic forecast variance of (8) at horizon $h = 1, ..., H$ constructed at $t = T$ be $g_{T+h|T}$. Then, it becomes*

$$g_{T+h|T} = D1_{T,h} + D2_{T,h}, \tag{9}$$

*uniformly in h where*

$$D1_{T,h} = h\sigma^2 \quad and\ D2_{T,h} = h^2\frac{\sigma^2}{T-1}. \tag{10}$$

Term $D1_{T,h}$ represents the variance of intrinsic future disturbances and increases at rate $h$ even for a large $T$ while $D2_{T,h}$ is the effect of parameter estimation which diminishes as $T$ increases. Under the Gaussian assumption on $\varepsilon_{T+h}$ in (2), the forecast interval becomes

$$\widetilde{y}_{T+h|T} \pm z_{\alpha/2}\sqrt{\hat{g}_{T+h|T}}, \tag{11}$$

where $\hat{g}_{T+h|T}$ is an estimate for $g_{T+h|T}$ and is constructed based on (9) and (10) with $\sigma^2$ replaced by $\widetilde{\sigma}^2 = \frac{1}{T-1}\sum_{t=2}^{T}(y_t - y_{t-1} - \widetilde{\beta})^2$.

### 3.3 Pretesting method

As we will investigate in Section 4 via Monte Carlo simulation, the forecast interval produced by the trend-stationary model suffers from undercoverage if $\rho$ is one or close to one; hence, the random walk model is useful although it contains a risk of providing an excessively large interval if $|\rho| < 1$. How to reconcile this dichotomy in the context of interval forecasting would be of interest.[5] However, in this study, we follow Ng and Vogelsang (2002) and take a simple approach to combine the two models by a unit root pretesting in the pre-crisis period.[6] Specifically, standard unit root tests of Dickey and Fuller (1979) or Phillips and Perron (1988) can be used with a model including intercept and time trend

$$\Delta y_t = \mu + \beta t + \phi y_{t-1} + \textstyle\sum_{j=1}^{d}\theta_j \Delta y_{t-j} + error, \tag{12}$$

for $t = d+2, ..., T$. The null hypothesis $H_0 : \phi = 0$ against an alternative hypothesis $H_1 : \phi < 0$ are tested. If $H_0$ is rejected then the trend-stationary model is used and otherwise the random walk model is used. Denote the variance of this pretesting forecast by

$$f^*_{T+h|T} = I_{p_{UR,T}<\alpha} f_{T+h|T} + (1 - I_{p_{UR,T}<\alpha}) g_{T+h|T},$$

where $I_{p_{UR,T}<\phi}$ is the indicator which takes one when the $p$-value of the unit root test ($p_{UR,T}$) is smaller than the pre-specified nominal level $\alpha$. The estimate for the variance is also denoted

[5] Canjels and Watson (1997) discussed an asymptotic approximation of the OLS and GLS estimators when $\rho$ is local to one. Vogelsang (1998) and Perron and Yabu (2009) provided a test for the trend slope parameter $\beta$ that is valid either when $|\rho| < 1$ or $\rho = 1$.

[6] Hansen (2010) introduced a model averaging in the same model but the AR parameter is local-to-unity. He proposes to average the estimators with weights determined by Mallows (1973) criterion, however, as far as we know, how to construct forecast interval for such an averaged forecast is still an open question.

by $\hat{f}^*_{T+h|T}$ and computed by

$$\hat{f}^*_{T+h|T} = I_{pUR,T<\alpha}\hat{f}_{T+h|T} + (1 - I_{pUR,T<\alpha})\hat{g}_{T+h|T}.$$

Note that this estimator is also interpreted as a shrinkage estimate of the forecast variance in which $\rho$ is shrunk to one when it is considered close to one. We investigate finite sample properties of this method in the following section via Monte Carlo simulation.

## 4 Testing and quantifying economic resilience

The forecasting interval discussed above can be plotted as a counterfactual alongside the actual output after the crisis. This illustrates information regarding whether the actual output has returned to the pre-crisis trajectory. A more formal approach is to formulate the null hypothesis that the actual value reached the counterfactual value $y^*_{T+h}$:

$$H_0 : y_{T+h} \geq y^*_{T+h}, \tag{13}$$

against the alternative hypothesis that the actual value remains below it

$$H_1 : y_{T+h} < y^*_{T+h}, \tag{14}$$

for $h = 1, 2, ..., H$. The following standardized test statistic is considered

$$s_h = \frac{y_{T+h} - \hat{y}^*_{T+h|T}}{\sqrt{\hat{f}^*_{T+h|T}}}. \tag{15}$$

This enables us to calculate the $p$-value at the $h$th horizon for the null hypothesis (13) against the alternative hypothesis (14). The null hypothesis is rejected if $\Phi(s_h) < \alpha$ where $\Phi(\cdot)$ is the cumulative standard normal distribution function and $\alpha$ is the level of significance. The first horizon at which $\Phi(s_h)$ exceeds $\alpha$ is considered the recovery date at the $100\alpha\%$ significance level. We can also directly plot $s_h$ for different economies so that their recovery patterns can be compared by using unit-free measures.[7]

Let us introduce two useful metrics constructed by $s_h$. The first metric measures the depth of the crisis. It can alternatively be interpreted as shock absorption as an economy experiencing a deep trough indicates low ability of shock absorption. To this end, we define the bottom of the test statistics by $s^* = \min_{1\leq h\leq h_0} s_h$ and the trough date by $k^* = \arg\min_{1\leq h\leq h_0} s_h$

[7] More precisely speaking, this method is subject to the multiple testing problem, as are many exercises of impulse response analyses. However, this issue is beyond the scope of this study.

where $h_0 < H$ is a certain horizon until which the bottom is experienced. This cutoff point $h_0$ is needed in practice because if the actual output keeps declining, no trough is identified.

The second measure pertains to cumulative recovery from the $k^*$th to the $H$th horizon. We define the following $RQ_H$ statistic:

$$RQ_H = 1 - \frac{-\sum_{h=k^*}^{H} s_h}{(H - k^*) \times |s^*|},$$

where $s^* < 0$. Note that if $s^* \geq 0$, no crisis effect is present and recovery is not defined. The denominator of the second term represents the total cumulative loss in a hypothetical economy with no recovery after the trough up to the $H$th horizon and the numerator computes the cumulative economic loss of the actual economy. Subtracting it from one gives a ratio of actual recovery to potential loss of no recovery. Figure 2 illustrates the concept of $RQ_H$ where the numerator and the denominator of the second term are depicted by the green area and by the sum of yellow and green areas, respectively, so that $RQ_H$ is the ratio of the yellow area to the sum of yellow and green areas. It becomes closer to zero or even negative when the economy lingers, while it may take a positive value close to one or even larger than one when the economy shows a quick recovery. In the latter case, we can judge that the economy is resilient. Furthermore, these measures also facilitate us to conduct cross-country comparisons, especially when the output is measured in different currency units.

## 5 Monte Carlo simulation

In this section, we conduct a Monte Carlo simulation to study finite sample properties of the proposed methods. The size and power of the test for (13) versus (14) are assessed by the coverage rate and the length of the forecast interval for simplicity, respectively. We consider the two-sided interval but in practice the one-sided test is used.

Throughout this section, the data is generated by the following model:

$$\begin{aligned} y_t &= \mu + \beta t + u_t, \\ u_t &= \rho u_{t-1} + \varepsilon_t, \end{aligned}$$

for $t = 1, ..., T + H$ where $u_0 \sim N(0, \sigma^2/(1 - \rho^2))$ when $|\rho| < 1$ and $u_0 = 0$ when $\rho = 1$. $\varepsilon_t$ is a quasi random variable drawn from the standard normal distribution independently for all $t$. In each replication, we use the generated data $y_t$ for $t = 1, ..., T$ and construct the 90% two-sided forecasting intervals by the trend-stationary model, the random walk model, and the pretesting method for $t = T + 1, ..., T + H$. The pretest is conducted by regression

(12) with the lag length selected by Ng and Perron (2001) and the 5% critical value is used as the decision rule. The number of replications is set at 5,000. We are interested in how the results vary with different values of $\rho$ especially when it is close to one, thus $\rho = \{0.0, 0.5, 0.8, 0.9, 0.95, 1.0\}$ is considered. We also investigate the effect of in-sample size by comparing results with $T = 50$, 100, 200. We set $\mu = 1$ and $\beta = 1$ for the entire simulations; however, these values do not qualitatively affect our conclusion. The results are presented at $h = 1, 10, 25, 50$.

The left four columns of Table 1 show the coverage rate when $T = 50$. The coverage rate of the trend-stationary model is close to the nominal level of 0.90 when $\rho$ is not larger than 0.5. However, it falls considerably below the nominal level as $\rho$ increases. Conversely, the coverage rate of the random walk model is very close to the nominal level when $\rho = 1$; however, it exceeds the nominal level as $\rho$ gets smaller and reaches one for long horizons. The pretesting method can compromise these models. When $\rho$ is not larger than 0.5, the coverage rate tracks that of the trend-stationary model. When $\rho$ is one, it is close to that of the random walk model. Otherwise, the coverage rate becomes some values between the trend-stationary and random walk models. Importantly, the coverage rate of the pretesting method is very close to the nominal level in all cases considered. Investigating the size is not sufficient as a correct size may be achieved at a cost of low power.

The right four columns of Table 1 show the average length of the forecasting interval over the replications. The length of the random walk forecast increases as the horizon increases regardless of $\rho$. The length of the trend-stationary forecast stays flat even when $h$ increases if $\rho \leq 0.5$, however, the interval widens as $h$ increases when $\rho$ is larger than 0.5. This reflects the effect of parameter estimation errors as pointed out by Sampson (1991) and Clements and Hendry (2001), although the effect may be understated because the forecast interval excessively undercovers for a large $\rho$. Similar to the coverage rate, the length of the pretesting method is very similar to that of the trend-stationary forecast when $\rho = 0.0$ or 0.5 and it is similar to the random walk forecast when $\rho$ is larger. Thus, the pretesting method must have a decent power.

The left four columns of Table 2 present the coverage rate when $T = 100$. It shows similar features to the case of $T = 50$; however, the coverage rates of the trend-stationary model and accordingly the pretesting method improve when $\rho < 1$ because the effect of parameter estimation errors is weakened with a larger $T$. We also conducted the same experiment with $T = 200$, but the results are very similar thus are not reported. The right four columns of Table 2 present the average lengths when $T = 100$. In the borderline case of $\rho = 0.8$,

the length of the pretesting method is more similar to the trend-stationary model than the random walk model, because the unit root test has a higher power. Because the former is shorter, a higher power is expected as $T$ increases. Also, the length of the trend-stationary model becomes even shorter as $T$ increases, because the effect of parameter estimation errors is reduced. The results when $T = 200$ are similar to those of $T = 100$ thus are not reported.

## 6 Empirical analysis

We use the natural logarithm of real GDP (in constant local currency prices, on a quarterly, seasonally adjusted basis) data spanning from 1995Q1 to 2023Q3 for 18 selected OECD countries[8]: Australia, Austria, Belgium, Canada, Denmark, Finland, France, Germany, Ireland, Italy, Japan, the Netherlands, Norway, Spain, Sweden, Switzerland, the United Kingdom, and the United States.[9] The data is sourced from the OECD Main Economic Indicator. Figure 3 illustrates that they commonly experienced a sudden drop and aftermath recovery during and after the GFC in 2007-2008 and the COVID-19 pandemic. In this section, we apply the proposed methods to scrutinize whether the GDP reattained its counterfactual pre-crisis growth trajectory. We also investigate whether shock absorption and recovery are heterogenous across different crises and countries. If so, we briefly explore how these characteristics are associated with potential determinants of economic resilience suggested by the existing literature (Duval and Vogel, 2008, Jollès et al., 2023).

With these objectives in mind, we first assess whether the economy has recovered its pre-crisis growth trajectory by plotting counterfactual forecast intervals after the GFC. We choose the crisis onset at 2008Q1 and use data from 1995Q1 to 2007Q4 for model estimation. The 90% two-sided forecast interval is constructed using the pretesting method from 2008Q1. In Figure 4, it is evident that, following the GFC, most countries did not manage to return to their pre-crisis growth trajectory at the 5% one-sided significance level, although exceptions include Germany, Japan, Norway, and Switzerland as they crossed the lower bound of the forecast interval. For the U.S. and Canada, the actual path runs almost parallel to the counterfactual trajectory, suggesting that the crisis influenced the level but not the growth rate of GDP. In several European countries, such as Spain and Italy, the actual GDP path further declined compared to the counterfactual forecast, resulting in decreases in both level

[8] Our sample consists of the same countries investigated by Duval and Vogel (2008) within the pool of 20 OECD countries minus New Zealand and Portugal. New Zealand is excluded due to the unavailability of several non-GDP variables crucial for the following analysis. Portugal is excluded because its real GDP series, characterized by an exceptionally smooth trend and a distinctive pattern.

[9] The real GDP data is available only after 1996Q1 in Italy and Netherland.

and growth rate. One may argue that this is caused by other subsequent shocks after the GFC such as the European sovereign debt crisis; however, disentangling these effects falls beyond the scope of our study. Figure 5 illustrates the counterfactual forecast after the COVID-19, with the crisis onset set at 2019Q3. We use data from 2010Q1 to 2019Q2 for model estimation. The figures generally show a deeper trough but faster recovery compared to the GFC. Interestingly, all countries, except for Austria, France, Germany, Japan, and the U.K., have re-established the pre-crisis growth path. It is also worth noting that the actual GDP level surpassed the point forecast in many countries such as Australia, Belgium, Denmark, Ireland, Italy, Netherlands, Norway, Sweden, and Switzerland.

The above observation is substantiated by the proposed absorption statistics ($s^*$) and the recovery statistics ($RQ_H$). We choose $H = 24$ up to 2013Q4 after the GFC and $H = 18$ up to 2023Q3 after the COVID-19, however, these specific choices do not affect our qualitative results. We set the maximum horizon by which the trough is determined $h_0 = 10$ in both cases. Table 3 provides a summary of these statistics for each country after the GFC and the COVID-19, respectively. For the GFC, the absorption statistic has mean -6.31 and the mean of recovery statistics is 0.23. For the COVID-19, the mean of absorption statistics (-13.24) is smaller, while the mean of the recovery statistics (0.82) is larger than the GFC. This suggests that the COVID-19 resulted in a more severe downturn followed by a faster recovery. Figure 6 plots the standardized test statistics (15) after the two crises for each country. The lines with black dots and white dots depict the GFC and the COVID-19, respectively, while the dotted line shows the critical value of the one-sided hypothesis at the 5% significance level. In most countries the standardized statistics after the GFC exhibit L-shape patterns and rarely crossed the critical value so that they were not resilient to the GFC shock and potential hysteresis effects are suggested. However, during the COVID-19 pandemic, deep declines were followed by a rapid increase and they exhibited V-shape patterns.

Our final agenda is to investigate the factors influencing the heterogeneity of resilience across different crises and countries. We select six factors pertaining to fiscal policies, financial leverage, innovation and technology, flexible labor markets, global connectivity, and inequality. We use data of general government debt outstanding per GDP, debt-to-equity ratio of financial corporations, country-level research and development (R&D) expenditures per GDP, the employment protection legislation (EPL) indicator published by the OECD, trade openness (the sum of exports and imports as a percentage of GDP), and the Gini index. Given the limitation of our sample to 18 countries, conducting a comprehensive analysis to identify the causal effects is challenging due to the presence of various confounding factors.

In this study, we solely present plots of bivariate regression lines, i.e. correlations.

Figure 7 illustrates the bivariate associations of our absorption and recovery measures with their potential determinants of economic resilience suggested by the literature. The left panels consider absorption and the right panels correspond to recovery. For panel A, the government debt ratio exhibits negative associations with both measures during the COVID-19, whereas the relations are opposite over the GFC. This contrast may arise because fiscal space was a more crucial characteristic during the COVID-19 in which government support was taken for granted, whereas government's involvement was more heterogenous and proxied by the debt outstanding. Panel B shows that financial leverage has a negative association with absorption and recovery in both crises. This is as expected and supported by existing literature. Note that panel B excludes Japan, as it is an influential observation with high financial leverage and relatively robust recovery and drives the entire relationship. Furthermore, panel C shows that the R&D spending has a positive association with both measures after the GFC but the relation is not clear during the COVID-19. In panel D, the EPL indicator ranging from 0 to 6 with a larger value indicating more strict regulation. The results are straightforward in that weaker regulation is associated with higher absorption and faster recovery. In panel E, greater trade openness aids in shock absorption in both crises, while its impact on recovery varies. After the GFC, the prolonged worldwide demand stagnation caused a slower recovery for more globally connected countries, while trade openness supported supply disruption and facilitated recovery after the COVID-19. Finally, panel F shows that inequality weakens absorption in both crises; however, its relation with recovery may seem opposite in the two crises. The GFC is characterized by damages to wealthy individuals who may gain relatively quicker recovery, while poorer individuals were affected more seriously and inequality may hinder recovery after the COVID-19. Overall, potential determinants such as financial leverage and labor market regulation may have negative correlations with shock absorption and recovery across the two crises; however, other factors vary in their associations, depending on the nature of the crisis. Note that the results are based on simple correlations with relatively small sample size and further investigations into these determinants will be an important focus for future research.

## 7 Conclusion

Motivated by the recent business cycle characteristics of a sharp drop and protracted recovery accentuated during the GFC and the COVID-19 pandemic, we proposed a formal testing procedure to investigate economic resilience based on a time-series counterfactual forecast-

ing interval of a linear trend with persistent noise model. It assesses whether the actual post-crisis output has returned to the counterfactual trajectory of no crisis. Our approach remains applicable even when a cross-section of control group is unavailable and circumvents potential bias in time-series regressions using data that includes structural breaks. It also has several advantages over the existing methods employed under similar motivation. Furthermore, we provide two useful measures pertaining to shock absorption and cumulative recovery. Our empirical investigation by using the log real GDP of 18 advanced countries reveals that most countries were not resilient to the GFC shock, while deep troughs were followed by fast recoveries after the COVID-19 pandemic and they exhibited V-shape patterns. We investigated the bivariate associations of these measures with potential determinants of economic resilience. Determinants such as the financial leverage and the labor market regulation have negative correlation with these measures; however, other factors vary in their associations, depending on the nature of the crisis.

While this endeavor hopefully inspires further research investigating economic resilience after global shocks, potential fields of applications extend beyond macroeconomics to include labor, regional, development and climate economics as well as political science. This study would also have spillover to various other disciplines such as ecology, psychology, sociology, environmental engineering, social engineering, and public health, to name a few. At the same time, we acknowledge several significant limitations. From an econometric perspective, our approach to reconciling trend-stationary and random walk forecasting models may be inadequate due to the bimodality in the sampling distribution of forecasting errors, as pointed out by Ng and Vogelsang (2002). The linear trend specification may be too simplistic to apply the method to various measures of interest. For example, the presence of structural changes in the trend function in the pre-crisis period must be carefully assessed for a more comprehensive empirical analysis. Secondly, from the viewpoint of causal inference, the effects of subsequent shocks during the post-crisis period must be ruled out. For example, the European Debt Crisis and Brexit must have affected those countries during the post-GFC crisis period so that the effects of the GFC may be overestimated. Nevertheless, this study should represent an initial step towards addressing the important and long-standing research objective of uncovering the economic resilience in an increasingly connected and heterogenous global economy.

## Appendix A. Proof of Theorems

**Proof of Theorem 1:** The forecasting error $\hat{\varepsilon}_{T+h} = y_{T+h} - \hat{y}_{T+h|T}$ is

$$\begin{aligned}
y_{T+h} - \hat{y}_{T+h|T} &= z'_{T+h}\delta + u_{T+h} - z'_{T+h}\hat{\delta} - \hat{\rho}^h(y_T - z'_T\hat{\delta}), \\
&= u_{T+h} + z'_{T+h}(\delta - \hat{\delta}) - \hat{\rho}^h(y_T - z'_T\hat{\delta}), \\
&= \textstyle\sum_{l=0}^{h-1} \rho^l \varepsilon_{T+h-l} + z'_{T+h}(\delta - \hat{\delta}) + \rho^h u_T - \hat{\rho}^h(y_T - z'_T\hat{\delta}), \\
&= \textstyle\sum_{l=0}^{h-1} \rho^l \varepsilon_{T+h-l} + z'_{T+h}(\delta - \hat{\delta}) + (\rho^h - \hat{\rho}^h) z_T(\delta - \hat{\delta}) \\
&\quad -\rho^h z_T(\delta - \hat{\delta}) + (\rho^h - \hat{\rho}^h)u_T, \\
&= \textstyle\sum_{l=0}^{h-1} \rho^l \varepsilon_{T+h-l} + (z_{T+h} - \rho^h z_T)'(\delta - \hat{\delta}) \\
&\quad +(\rho^h - \hat{\rho}^h)u_T + (\rho^h - \hat{\rho}^h)z'_T(\delta - \hat{\delta}), \\
&= I + II + III + IV,
\end{aligned}$$

uniformly in $h$. We now consider the variance of $\hat{\varepsilon}_{T+h}$. Because $\hat{\delta}$ and $\hat{\rho}$ are asymptotically independent as the information matrix is block diagonal, $ACov(I, II) = ACov(I, IV) = ACov(II, III) = ACov(III, IV) = 0$. Therefore,

$$AVar(\hat{\varepsilon}_{T+h|T}) \equiv f_{T+h|T} = AVar(I) + AVar(II) + AVar(III) + AVar(IV),$$

where

$$\begin{aligned}
AVar(I) &= \sigma^2 \textstyle\sum_{l=0}^{h-1} \rho^{2l} \equiv C1_{T,h}, \\
AVar(II) &= (z_{T+h} - \rho^h z_T)' AVar(\hat{\delta})(z_{T+h} - \rho^h z_T) \equiv C2_{T,h}.
\end{aligned}$$

For $AVar(III)$ and $AVar(IV)$, we obtain

$$\begin{aligned}
AVar(III) &= u_T^2 \times AVar(\hat{\rho}^h) \equiv C3_{T,h}, \\
AVar(IV) &= AVar(\hat{\rho}^h) \times z'_T AVar(\hat{\delta}) z_T \equiv C4_{T,h},
\end{aligned}$$

which completes the proof.■

**Proof of Theorem 2:** When $\rho = 1$, the forecast error becomes

$$\begin{aligned}
\widetilde{\varepsilon}_{T+h|T} &= y_{T+h} - \widetilde{y}_{T+h|T}, \\
&= y_T + h\beta + \textstyle\sum_{l=0}^{h-1} \varepsilon_{T+h-l} - y_T - h\widetilde{\beta}, \\
&= \textstyle\sum_{l=0}^{h-1} \varepsilon_{T+h-l} + h(\beta - \widetilde{\beta}), \\
&= I + II,
\end{aligned}$$

uniformly in $h$. Because $I$ and $II$ are independent,

$$AVar(\widetilde{\varepsilon}_{T+h|T}) \equiv g_{T+h|T} = AVar(I) + AVar(II),$$

where

$$AVar(I) = h\sigma^2 \equiv D1_{T,h},$$

and

$$AVar(II) = h^2 \frac{\sigma^2}{T-1} \equiv D2_{T,h},$$

which completes the proof.■

## Appendix B. Comparison between FGLS and OLS forecast intervals

In this Appendix, we compare the coverage properties of the forecasting interval produced by the best linear unbiased prediction estimated by the Prais-Winsten FGLS with the forecasting interval produced by Durbin's regression estimated using the OLS. We also investigate the coverage properties of the pretesting method. Durbin's regression reparametrizes models (1) and (2) by subtracting the lagged equation multiplied by $\rho$ from model (1):

$$y_t - \rho y_{t-1} = \mu(1-\rho) + \beta[t - \rho(t-1)] + \varepsilon_t,$$

or

$$\begin{aligned} y_t &= \mu^* + \beta^* t + \rho y_{t-1} + \varepsilon_t, \\ &= x_t'\theta + \varepsilon_t, \end{aligned} \tag{A.1}$$

where $\mu^* \equiv \mu(1-\rho) + \beta\rho$, $\beta^* \equiv \beta(1-\rho)$, $x_t \equiv [1, t, y_{t-1}]'$ and $\theta \equiv [\mu^*, \beta^*, \rho]'$. Because model (A.1) has spherical errors $\varepsilon_t$, the OLS estimation gives the efficient estimator for the pseudo-true coefficient $\theta$. By using matrix notations $X = [x_2, ..., x_T]'$, $y = [y_2, ..., y_T]'$ and $\varepsilon = [\varepsilon_2, ..., \varepsilon_T]'$, (A.1) is written as

$$y = X\theta + \varepsilon.$$

The OLS estimator for the pseudo-true coefficients and their covariance matrix are given by $\check{\theta} \equiv [\check{\mu}^*, \check{\beta}^*, \check{\rho}]' = (X'X)^{-1}X'y$ and $\sigma^2(X'X)^{-1}$, respectively.

Let $\check{x}_{T+h|T} = [1, T+h, \check{y}_{T+h-1|T}]'$ for $h = 1, 2, ...$ where $\check{y}_{T|T} = y_T$. The $h$ period ahead forecast is recursively constructed by

$$\begin{aligned} \check{y}_{T+h|T} &= \check{\mu}^* + \check{\beta}^*(T+h) + \check{\rho}\check{y}_{T+h-1|T}, \\ &= \check{x}_{T+h|T}'\check{\theta}. \end{aligned} \tag{A.2}$$

As shown in Appendix C, the forecasting error $\check{\varepsilon}_{T+h|T} = y_{T+h} - \check{y}_{T+h|T}$ becomes

$$\begin{aligned} y_{T+h} - \check{y}_{T+h|T} &= x_{T+h}'\theta + \varepsilon_{T+h} - \check{x}_{T+h|T}'\check{\theta}, \\ &= \textstyle\sum_{l=0}^{h-1} \rho^l \varepsilon_{T+h-l} + \sum_{l=0}^{h-1} \rho^l x_{T+h-l}'(\theta - \check{\theta}) \\ &\quad + \textstyle\sum_{l=0}^{h-1} (\check{\rho}^l - \rho^l)\varepsilon_{T+h-l} + \sum_{l=0}^{h-1} (\check{\rho}^l - \rho^l) x_{T+h-l}'(\theta - \check{\theta}). \end{aligned} \tag{A.3}$$

Based on this expression, the following result for the asymptotic variance of forecasting error of the Durbin's regression model is obtained.

**Theorem A** *Suppose $y_t$ for $t = 1, ..., T+H$ is generated by (1) and (2) with $|\rho| < 1$. Let the asymptotic forecast error variance of (A.3) at a horizon $h = 1, ..., H$ constructed at $t = T$ be $b_{T+h|T}$. Then,*

$$b_{T+h|T} = B1_{T,h} + B2_{T,h} + B3_{T,h} + B4_{T,h}, \tag{A.4}$$

*uniformly in $h$ where*

$$\begin{aligned} B1_{T,h} &= \sigma^2 \textstyle\sum_{l=0}^{h-1} \rho^{2l}, \\ B2_{T,h} &= \textstyle\sum_{l=0}^{h-1} \sum_{k=0}^{h-1} \rho^{l+k} x_{T+h-l}' AVar(\check{\theta}) x_{T+h-k}, \\ B3_{T,h} &= \sigma^2 \textstyle\sum_{l=0}^{h-1} AVar(\check{\rho}^l), \\ B4_{T,h} &= \textstyle\sum_{l=0}^{h-1} \sum_{k=0}^{h-1} ACov(\check{\rho}^l, \check{\rho}^k) x_{T+h-l}' AVar(\check{\theta}) x_{T+h-k}. \end{aligned}$$

See Appendix C for a proof. The forecast interval can be constructed by

$$\check{y}_{T+h|T} \pm z_{\alpha/2}\sqrt{\check{b}_{T+h|T}},$$

where $\check{b}_{T+h|T}$ is an estimate of $b_{T+h|T}$ by plugging $\widetilde{AVar}(\check{\theta}) = \check{\sigma}^2(X'X)^{-1}$ with $\check{\sigma}^2 = (y - X\check{\theta})'(y - X\check{\theta})/T$, $\widetilde{AVar}(\check{\rho}^l) = l^2\check{\rho}^{2(l-1)}\widetilde{AVar}(\check{\rho})$ with $\check{\rho}$ is the OLS estimator, $\widetilde{ACov}(\check{\rho}^l, \check{\rho}^k) = lk\check{\rho}^{\{(l-1)+(k-1)\}}\widetilde{AVar}(\check{\rho})$ with $\widetilde{AVar}(\check{\rho}) = \frac{1-\check{\rho}^2}{T}$ by using the delta method.

In the following, we conduct a Monte Carlo simulation under the same setup as in Section 4 to compare the above method (denoted by TS-OLS in tables) and Prais-Winsten FGLS (denoted by TS-FGLS) as well as their pretesting versions (denoted by PT-OLS and PT-FGLS, respectively). Table A1-a gives the results when $T = 50$. The coverage rate of TS-OLS is very close to the nominal level 0.90 when $\rho = 0.0$ and 0.5; however, it shows significant undercoverage as $\rho$ becomes large. This feature is shared with TS-FGLS, although the undercoverage is somewhat more severe. As a result, the average length of TS-OLS is larger than TS-FGLS. In either case, the coverage rates of solely using trend-stationary models are too low. If we use the pretesting version, PT-OLS gives much better coverage rate for larger values of $\rho$. This also occurs with the pretesting method using the FGLS (PT-FGLS) investigated in Section 4. A slight difference can be seen in the average length, in which PT-FGLS yields a little tighter interval than PT-OLS. Table A1-b provides the results when $T = 100$. Again, the coverage rate of TS-OLS is a little better than the TS-FGLS; however, they are too low. The coverage rate becomes very close to the nominal level for both methods when pretesting is involved. The length of PT-OLS is somewhat larger than PT-FGLS. Therefore, this justifies our use of the pretesting version of Prais-Winsten FGLS in our main analysis.

## Appendix C. Proof of Theorem A

The forecasting error $\check{\varepsilon}_{T+h|T} = y_{T+h} - \check{y}_{T+h|T}$ of the Durbin's regression model is

$$\begin{aligned} y_{T+h} - \check{y}_{T+h|T} &= x'_{T+h}\theta + \varepsilon_{T+h} - \check{x}'_{T+h|T}\hat{\theta}, \\ &= x'_{T+h}\theta + \varepsilon_{T+h} - x'_{T+h}\hat{\theta} + (x'_{T+h} - \check{x}'_{T+h|T})\hat{\theta}, \\ &= x'_{T+h}(\theta - \check{\theta}) + \hat{\rho}(y_{T+h-1} - \check{y}_{T+h-1|T}) + \varepsilon_{T+h}, \end{aligned} \tag{A.5}$$

for $h = 1, 2, ...H$ uniformly in $h$, because

$$\begin{aligned} (x'_{T+h} - \check{x}'_{T+h|T})\hat{\theta} &= [0\ 0\ y_{T+h-1} - \check{y}_{T+h-1|T}] \begin{bmatrix} \check{\mu}^* \\ \check{\beta}^* \\ \check{\rho} \end{bmatrix}, \\ &= \check{\rho}(y_{T+h-1} - \check{y}_{T+h-1|T}). \end{aligned}$$

The second term of (A.5) has a lag of $\check{\varepsilon}_{T+h|T}$ or $\check{\varepsilon}_{T+h-1|T} = y_{T+h-1} - \check{y}_{T+h-1|T}$. Recursively plugging a lag of (A.5) will yield,

$$\begin{aligned} y_{T+h} - \check{y}_{T+h|T} &= x'_{T+h}(\theta - \check{\theta}) + \check{\rho}\{x'_{T+h-1}(\theta - \check{\theta}) + \check{\rho}(y_{T+h-2} - \check{y}_{T+h-2|T}) + \varepsilon_{T+h-1}\} + \varepsilon_{T+h}, \\ &= x'_{T+h}(\theta - \check{\theta}) + \check{\rho}x'_{T+h-1}(\theta - \check{\theta}) + \check{\rho}^2 x'_{T+h-2}(\theta - \check{\theta}) \\ &\quad + \cdots + \check{\rho}^{h-1}x'_{T+1}(\theta - \check{\theta}) + \check{\rho}^h(y_T - y_T) \\ &\quad + \varepsilon_{T+h} + \check{\rho}\varepsilon_{T+h-1} + \check{\rho}^2\varepsilon_{T+h-2} + \cdots + \check{\rho}^{h-1}\varepsilon_{T+1}, \\ &= \textstyle\sum_{l=0}^{h-1} \check{\rho}^l \varepsilon_{T+h-l} + \sum_{j=0}^{h-1} \check{\rho}^l x'_{T+h-l}(\theta - \check{\theta}), \\ &= \textstyle\sum_{l=0}^{h-1} \rho^l \varepsilon_{T+h-l} + \sum_{l=0}^{h-1} \rho^l x'_{T+h-l}(\theta - \check{\theta}) \\ &\quad + \textstyle\sum_{l=0}^{h-1} (\check{\rho}^l - \rho^l)\varepsilon_{T+h-l} + \sum_{l=0}^{h-1} (\check{\rho}^l - \rho^l) x'_{T+h-l}(\theta - \check{\theta}), \\ &= I + II + III + IV. \end{aligned}$$

We now consider the variance of $\check{\varepsilon}_{T+h|T}$. Because $\check{\theta}$ and $\varepsilon_{T+l}$ for $l \geq 1$ are independent, $ACov(I, II) = ACov(I, IV) = ACov(II, III) = ACov(III, IV) = 0$. Furthermore, if we use a consistent estimate $\widetilde{\rho}$ for $\rho$, $ACov(I, III) = ACov(II, IV) = 0$. Therefore,

$$AVar(\hat{\varepsilon}_{T+h|T}) \equiv b_{T+h|T} = AVar(I) + AVar(II) + AVar(III) + AVar(IV),$$

where

$$\begin{aligned} AVar(I) &= \sigma^2 \textstyle\sum_{l=0}^{h-1} \rho^{2l} \equiv B1_{T,h}, \\ AVar(II) &= \textstyle\sum_{l=0}^{h-1} \sum_{k=0}^{h-1} \rho^l x'_{T+h-l} AVar(\check{\theta}) x_{T+h-k} \rho^k \equiv B2_{T,h}. \end{aligned}$$

For $AVar(III)$ and $AVar(IV)$, we obtain

$$\begin{aligned} AVar(III) &= \sigma^2 \textstyle\sum_{l=0}^{h-1} AVar(\check{\rho}^l) \equiv B3_{T,h}, \\ AVar(IV) &= \sigma^2 \textstyle\sum_{l=0}^{h-1} \sum_{k=0}^{h-1} ACov(\check{\rho}^l, \check{\rho}^k) x'_{T+h-l} AVar(\check{\theta}) x_{T+h-k} \equiv B4_{T,h}, \end{aligned}$$

which completes the proof.■

## References


Abadie, A. and Gardeazabal, J. (2003), "The Economic Costs of Conflict: A Case Study of the Basque Country," *American Economic Review* 93, 113-132.

Abadie, A., Diamond, A., and Hainmueller, J. (2010), "Synthetic Control Methods for Comparative Case Studies: Estimating the Effects of California's Tobacco Control Program," *Journal of the American Statistical Association* 105, 493-505.

Acemoglu, D. and Scott, A. (1997), "Asymmetric Business Cycles: Theory and Time-Series Evidence," *Journal of Monetary Economics* 40(3), 501-533.

Aikman, D., Drehmann, M., Juselius, M., and Xing, X. (2022), "The Scarring Effects of Deep Contractions," BIS Working Paper, 1043.

Bai, J. and Ng, S. (2005), "Tests for Skewness, Kurtosis, and Normality for Time Series Data," *Journal of Business & Economic Statistics* 23(1), 49-60.

Ball, L. M. (2014), "Long-term Damage from the Great Recession in OECD Countries," NBER Working Paper 20185.

Blanchard, O. and Summers, L. H. (1987), "Hysteresis in Unemployment," *European Economic Review* 31, 288-295.

Blanchard, O., Cerutti, E., and Summers, L. H. (2015), "Inflation Activity - Two Explorations and Their Monetary Policy Implications," IMF Working Paper 15/230.

Briguglio, L., Cordina, G., Farrugia, N., and Vella, S. (2009), "Economic Vulnerability and Resilience: Concepts and Measurements," *Oxford Development Studies* 37(3), 229-247.

Campbell, J. Y. and Mankiw, N. G. (1987), "Are Output Fluctuations Transitory?" *The Quarterly Journal of Economics* 102(4), 857-880.

Canjels, E. and Watson, M. W. (1997), "Estimating Deterministic Trends in the Presence of Serially Correlated Errors," *The Review of Economics and Statistics* 79, 184-200.

Cavallo, E., Galiani, S., Noy, I., and Pantano, J. (2013), "Catastrophic Natural Disasters and Economic Growth," *The Review of Economics and Statistics* 95(5), 1549-1561.

Cerra, V. and Saxena, S. C. (2008), "Growth Dynamics: The Myth of Economic Recovery," *American Economic Review* 98(1), 439-457.

Cerra, V., Fatás, A., and Saxena, S. C. (2023), "Hysteresis and Business Cycles," *Journal of Economic Literature* 61(1), 181-225.

Clements, M. P. and Hendry, D. F. (2001), "Forecasting with Differenced-Stationary and Trend-Stationary Models," *The Econometrics Journal* 4(1), S1-S19.

Clements, M. P. and Krolzig, H-M. (2003), "Business Cycle Asymmetries: Characterization and Testing Based on Markov-Switching Autoregressions," *Journal of Business and Economic Statistics* 21(1), 196-211.

De Long, J. B. and Summers, L. H. (1984), "Are Business Cycles Symmetric?" Technical report, National Bureau of Economic Research.

Dickey, D. and Fuller, W. (1979), "Distribution of the Estimators for Autoregressive Time Series with a Unit Root," *Journal of the American Statistical Association* 74, 427-431.

Diop, S., Asongu, S. A., and Nnanna, J. (2021), "COVID-19 Economic Vulnerability and Resilience Indexes: Global Evidence," *International Social Science Journal* 71(S1), 37-50.

Duval, R. and Vogel, L. (2008), "Economic Resilience to Shocks: The Role of Structural Policies," *OECD Economic Studies* 44.

Falk, B. and Roy, A. (2005), "Forecasting Using the Trend Model with Autoregressive Errors," *International Journal of Forecasting* 21, 291-302.

Fingleton, B., Garretsen, H., and Martin, R. (2012), "Recessionary Shocks and Regional Employment: Evidence on the Resilience of U.K. Regions," *Journal of Regional Science* 52(1), 109-133.

Goldberger, A. S. (1962), "Best Linear Unbiased Prediction in the Generalized Linear Regression Model," *Journal of the American Statistical Association* 57(298), 369-375.

Hamilton, J. D. (1989), "A New Approach to the Economic Analysis of Nonstationary Time Series and the Business Cycle," *Econometrica* 57(2), 357-384.

Hansen, B. E. (2010), "Averaging Estimators for Autoregressions with a Near Unit Root," *Journal of Econometrics* 158, 142-155.

Iseringhausen, M., Petrella, I., and Theodoridis, K. (2023), "Aggregate Skewness and the Business Cycle," forthcoming in *The Review of Economics and Statistics*.

Jensen, H., Petrella, I., Ravn, S. H., and Santoro, E. (2020), "Leverage and Deepening Business-Cycle Skewness," *American Economic Journal: Macroeconomics* 12(1), 245-281.

Jollès, M., Meyermans, E., and Vašíček, B. (2023), "Determinants of Macroeconomic Resilience in the Euro Area: An Empirical Assessment of National Policy Levers," *Economic Systems* 47, 101093.

Mallows, C. L. (1973), "Some Comments on $C_p$," *Technometrics* 15, 661-675.

Martin, R. (2012), "Regional Economic Resilience, Hysteresis and Recessionary Shocks," *Journal of Economic Geography* 12, 1-32.

Morley, J. and Piger, J. (2012), "The Asymmetric Business Cycle," *The Review of Economics and Statistics* 94(1), 208-221.

Neftci, S. N. (1984), "Are Economic Time Series Asymmetric Over the Business Cycle?" *Journal of Political Economy* 92(2), 307-328.

Nelson, C. R. and Plosser, C. (1982), "Trends and Random Walks in Macroeconomic Time Series: Some Evidence and Implications," *Journal of Monetary Economics* 10, 139-162.

Ng, S. and Perron, P. (2001), "Lag Length Selection and the Construction of Unit Root Tests With Good Size and Power," *Econometrica* 69(6), 1519-1554.

Ng, S. and Vogelsang, T.J. (2002), "Forecasting Autoregressive Time Series in the Presence of Deterministic Components," *Econometrics Journal* 5, 196-224.

Noy, I. and Yonson, R. (2018), "Economic Vulnerability and Resilience to Natural Hazards: A Survey of Concepts and Measurements," *Sustainability.*

Perron, P. (1989), "The Great Crash, the Oil Price Shock, and the Unit Root Hypothesis," *Econometrica* 57,(6), 1361-1401.

Perron, P. and Yabu, T. (2009), "Estimating Deterministic Trends With an Integrated or Stationary Noise Component," *Journal of Econometrics* 151, 56-69.

Phillips, P.C.B. and Perron, P. (1988), "Testing for a Unit Root in Time Series Regression," *Biometrika* 75, 335-346.

Plagborg-Møller, M., Reichlin, L., Ricco, G., and Hasenzagl, T. (2020), "When is Growth at Risk?" *Brooking Papers on Economic Activity*, 167-213.

Prais, S. and Winsten, C. (1954), "Trend Estimation and Serial Correlation," Cowles Commission Discussion Paper No. 383, Chicago.

Reinhart, C. M. and Rogoff, K. S. (2014), "Recovery from Financial Crises: Evidence from 100 Episodes," *American Economic Review* 104(5), 50-55.

Roy, A. and Fuller, W. A. (2001), "Estimation for Autoregressive Processes with a Root Near One," *Journal of Business and Economic Statistics* 19, 482-493.

Sampson, M. (1991), "The Effect of Parameter Uncertainty on Forecast Variance for Unit Root and Trend Stationary Time-Series Models," *Journal of Applied Econometrics* 6(1), 67-76.

Stock, J. H. (1991), "Confidence Intervals for the Largest Autoregressive Root in U.S. Macroeconomic Time Series," *Journal of Monetary Economics* 28(3), 435-459.

Vogelsang, T. J. (1998), "Trend Function Hypothesis Testing in the Presence of Serial Correlation," *Econometrica* 66(1), 123-148.

**Figure 1. Patterns of Recovery**

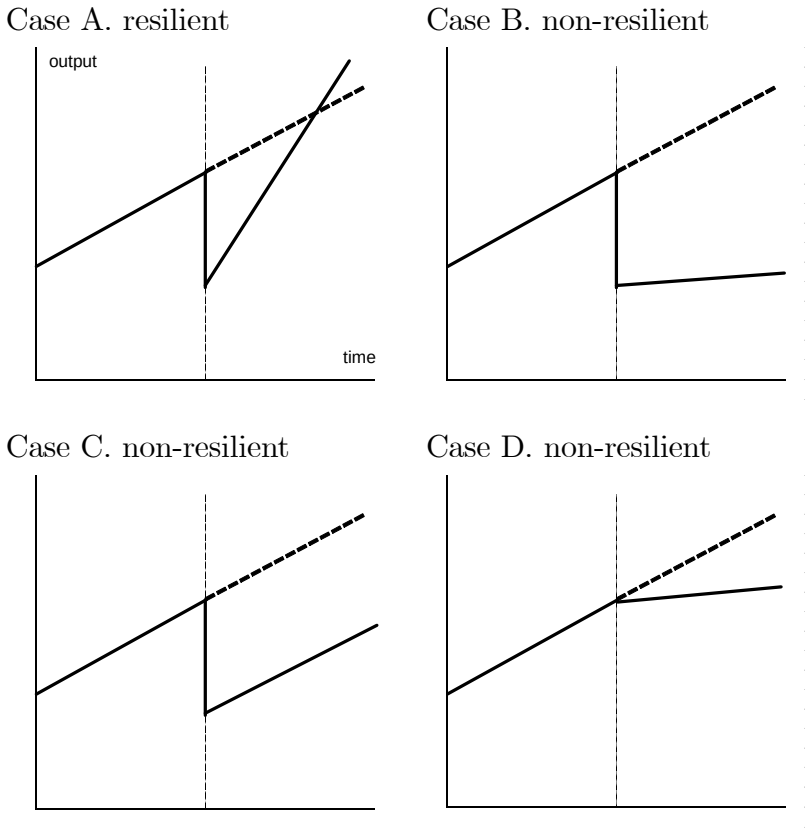


**Figure 2. The $RQ_H$ Statistic of Cumulative Recovery**

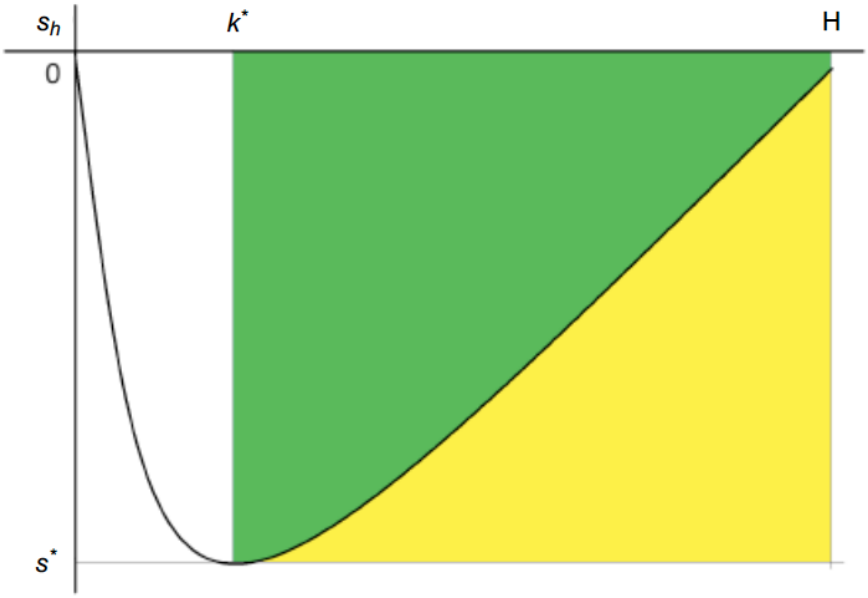

**Table 1. Coverage Rate and Average Length of Forecast Intervals ($T = 50$)**

| | Coverage rate | | | | Average length | | | |
|---|---|---|---|---|---|---|---|---|
| | *h=1* | *h=10* | *h=25* | *h=50* | *h=1* | *h=10* | *h=25* | *h=50* |
| *ρ=0.0* | | | | | | | | |
| TS | 0.90 | 0.89 | 0.90 | 0.90 | 3.42 | 3.50 | 3.68 | 4.09 |
| RW | 0.91 | 1.00 | 1.00 | 1.00 | 4.73 | 16.24 | 28.76 | 47.05 |
| PT | 0.90 | 0.89 | 0.90 | 0.90 | 3.42 | 3.50 | 3.68 | 4.09 |
| *ρ=0.5* | | | | | | | | |
| TS | 0.88 | 0.87 | 0.85 | 0.85 | 3.39 | 4.17 | 4.62 | 5.57 |
| RW | 0.90 | 1.00 | 1.00 | 1.00 | 3.84 | 13.18 | 23.34 | 38.19 |
| PT | 0.88 | 0.87 | 0.86 | 0.86 | 3.41 | 4.94 | 6.31 | 8.56 |
| *ρ=0.8* | | | | | | | | |
| TS | 0.89 | 0.78 | 0.78 | 0.76 | 3.39 | 5.87 | 6.96 | 8.92 |
| RW | 0.90 | 0.98 | 1.00 | 1.00 | 3.52 | 12.08 | 21.39 | 34.99 |
| PT | 0.89 | 0.91 | 0.92 | 0.91 | 3.45 | 10.50 | 18.04 | 29.13 |
| *ρ=0.9* | | | | | | | | |
| TS | 0.89 | 0.75 | 0.68 | 0.67 | 3.37 | 6.90 | 8.62 | 11.32 |
| RW | 0.90 | 0.95 | 0.98 | 1.00 | 3.42 | 11.76 | 20.82 | 34.05 |
| PT | 0.90 | 0.91 | 0.94 | 0.95 | 3.40 | 11.10 | 19.41 | 31.59 |
| *ρ=0.95* | | | | | | | | |
| TS | 0.89 | 0.72 | 0.62 | 0.58 | 3.35 | 7.51 | 9.73 | 12.95 |
| RW | 0.90 | 0.93 | 0.95 | 0.97 | 3.37 | 11.58 | 20.50 | 33.53 |
| PT | 0.90 | 0.90 | 0.91 | 0.93 | 3.35 | 11.15 | 19.59 | 31.94 |
| *ρ=1.0* | | | | | | | | |
| TS | 0.88 | 0.68 | 0.54 | 0.47 | 3.29 | 7.65 | 10.10 | 13.55 |
| RW | 0.90 | 0.90 | 0.89 | 0.90 | 3.30 | 11.34 | 20.09 | 32.86 |
| PT | 0.89 | 0.87 | 0.86 | 0.86 | 3.29 | 10.97 | 19.29 | 31.46 |

**Table 2. Coverage Rate and Average Length of Forecast Intervals ($T = 100$)**

| | Coverage rate | | | | Average length | | | |
|---|---|---|---|---|---|---|---|---|
| | *h=1* | *h=10* | *h=25* | *h=50* | *h=1* | *h=10* | *h=25* | *h=50* |
| *ρ=0.0* | | | | | | | | |
| TS | 0.89 | 0.91 | 0.90 | 0.89 | 3.35 | 3.36 | 3.40 | 3.48 |
| RW | 0.90 | 1.00 | 1.00 | 1.00 | 4.68 | 15.45 | 26.06 | 40.40 |
| PT | 0.89 | 0.91 | 0.90 | 0.89 | 3.35 | 3.36 | 3.40 | 3.48 |
| *ρ=0.5* | | | | | | | | |
| TS | 0.89 | 0.89 | 0.89 | 0.88 | 3.34 | 3.96 | 4.08 | 4.31 |
| RW | 0.90 | 1.00 | 1.00 | 1.00 | 3.82 | 12.62 | 21.28 | 32.99 |
| PT | 0.89 | 0.89 | 0.89 | 0.88 | 3.34 | 3.96 | 4.08 | 4.31 |
| *ρ=0.8* | | | | | | | | |
| TS | 0.89 | 0.84 | 0.85 | 0.84 | 3.34 | 5.70 | 6.14 | 6.80 |
| RW | 0.89 | 0.98 | 1.00 | 1.00 | 3.49 | 11.53 | 19.45 | 30.15 |
| PT | 0.88 | 0.87 | 0.87 | 0.87 | 3.37 | 7.35 | 10.24 | 14.22 |
| *ρ=0.9* | | | | | | | | |
| TS | 0.90 | 0.82 | 0.79 | 0.77 | 3.34 | 7.13 | 8.27 | 9.50 |
| RW | 0.91 | 0.96 | 0.99 | 1.00 | 3.40 | 11.23 | 18.94 | 29.37 |
| PT | 0.90 | 0.91 | 0.92 | 0.93 | 3.37 | 10.11 | 16.40 | 24.91 |
| *ρ=0.95* | | | | | | | | |
| TS | 0.89 | 0.79 | 0.73 | 0.68 | 3.33 | 8.06 | 10.03 | 11.96 |
| RW | 0.90 | 0.93 | 0.96 | 0.99 | 3.36 | 11.08 | 18.68 | 28.96 |
| PT | 0.90 | 0.90 | 0.92 | 0.94 | 3.34 | 10.61 | 17.62 | 27.09 |
| *ρ=1.0* | | | | | | | | |
| TS | 0.89 | 0.76 | 0.65 | 0.55 | 3.29 | 8.71 | 11.62 | 14.48 |
| RW | 0.90 | 0.89 | 0.90 | 0.90 | 3.30 | 10.88 | 18.35 | 28.44 |
| PT | 0.90 | 0.88 | 0.87 | 0.86 | 3.29 | 10.60 | 17.69 | 27.29 |

**Figure 3. Log Real GDP: From 1995Q1 to 2023Q3**

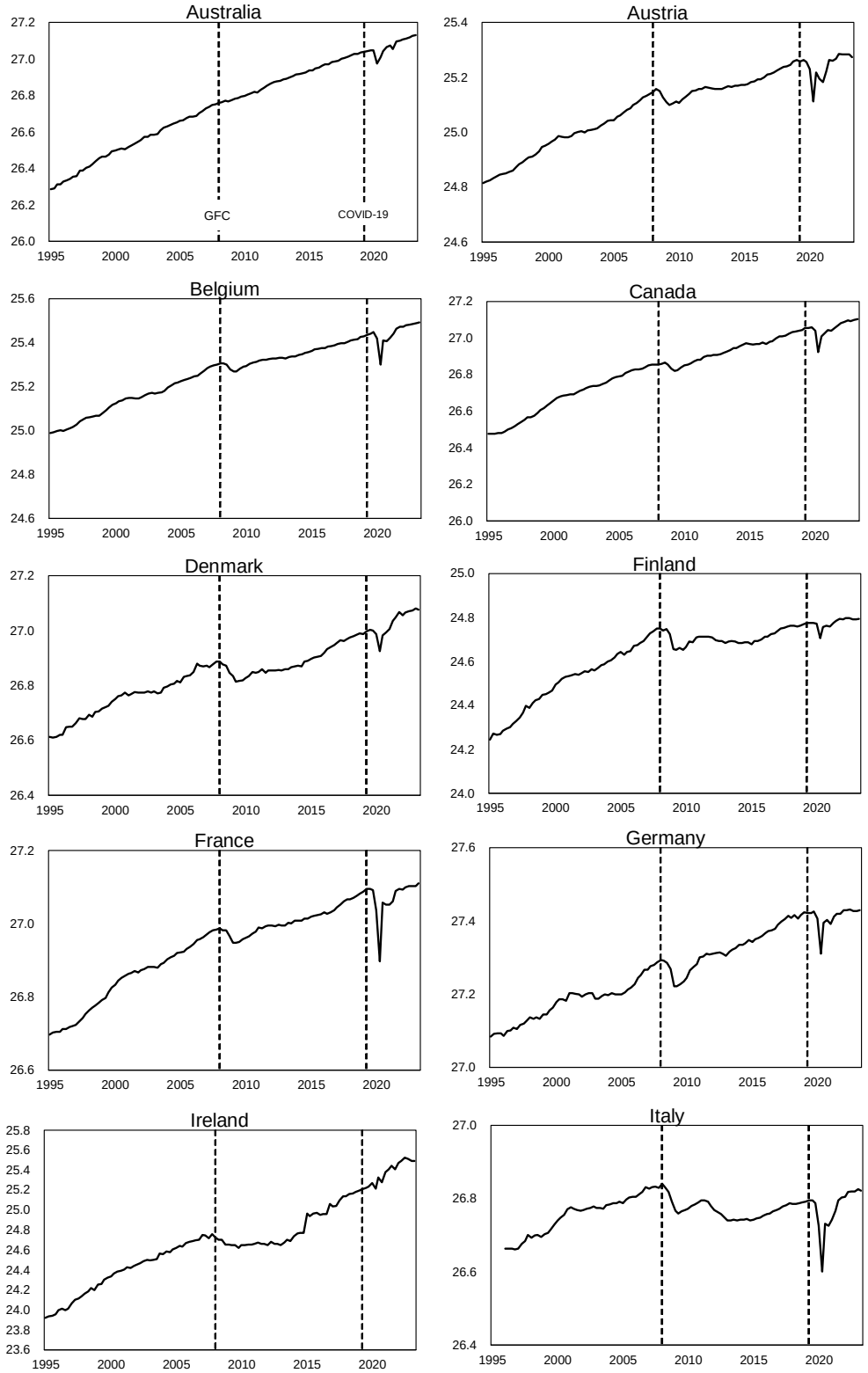

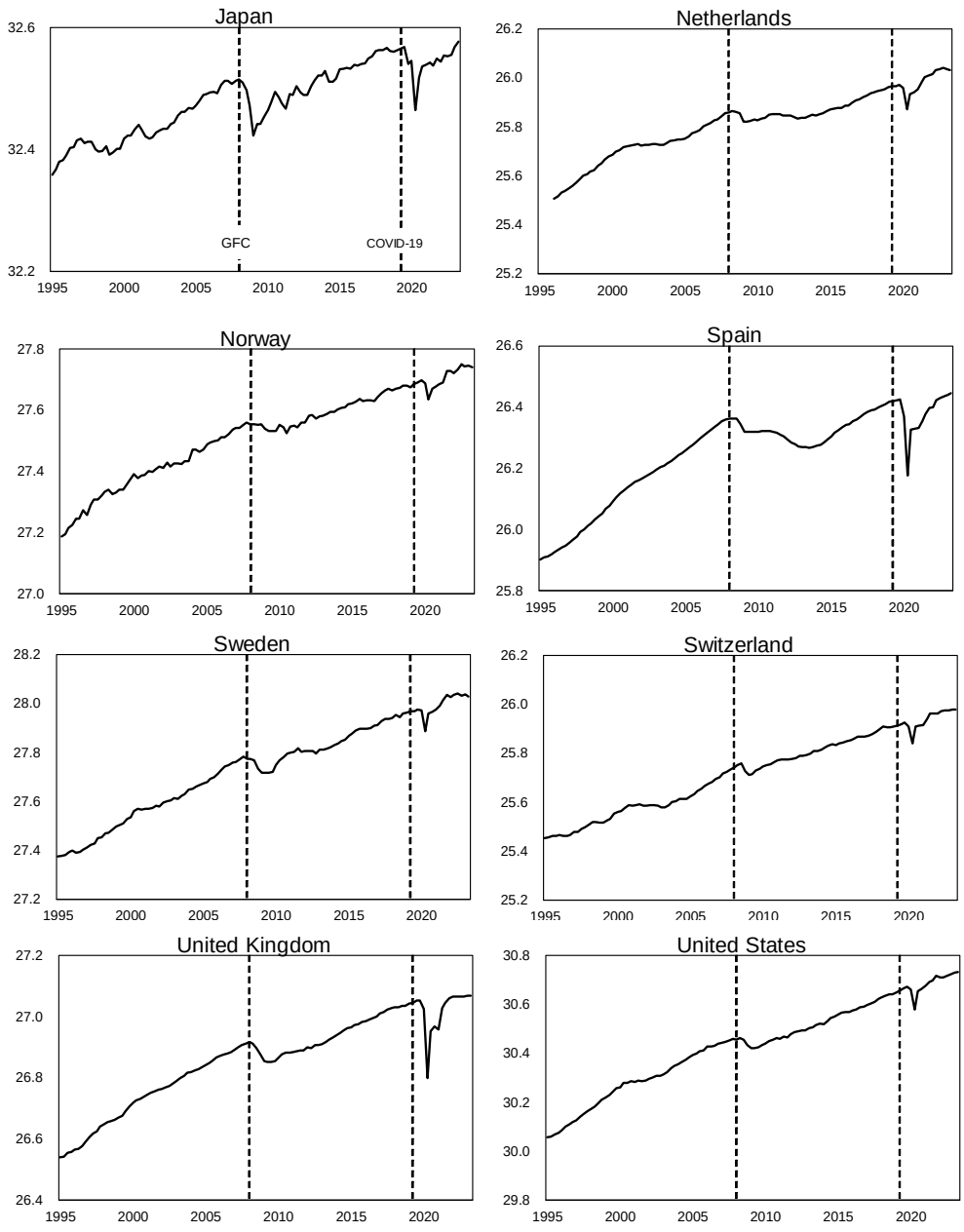
Japan
GFC
COVID-19
Netherlands
Norway
Spain
Sweden
Switzerland
United Kingdom
United States

**Figure 4. Counterfactual Forecast Interval after GFC**

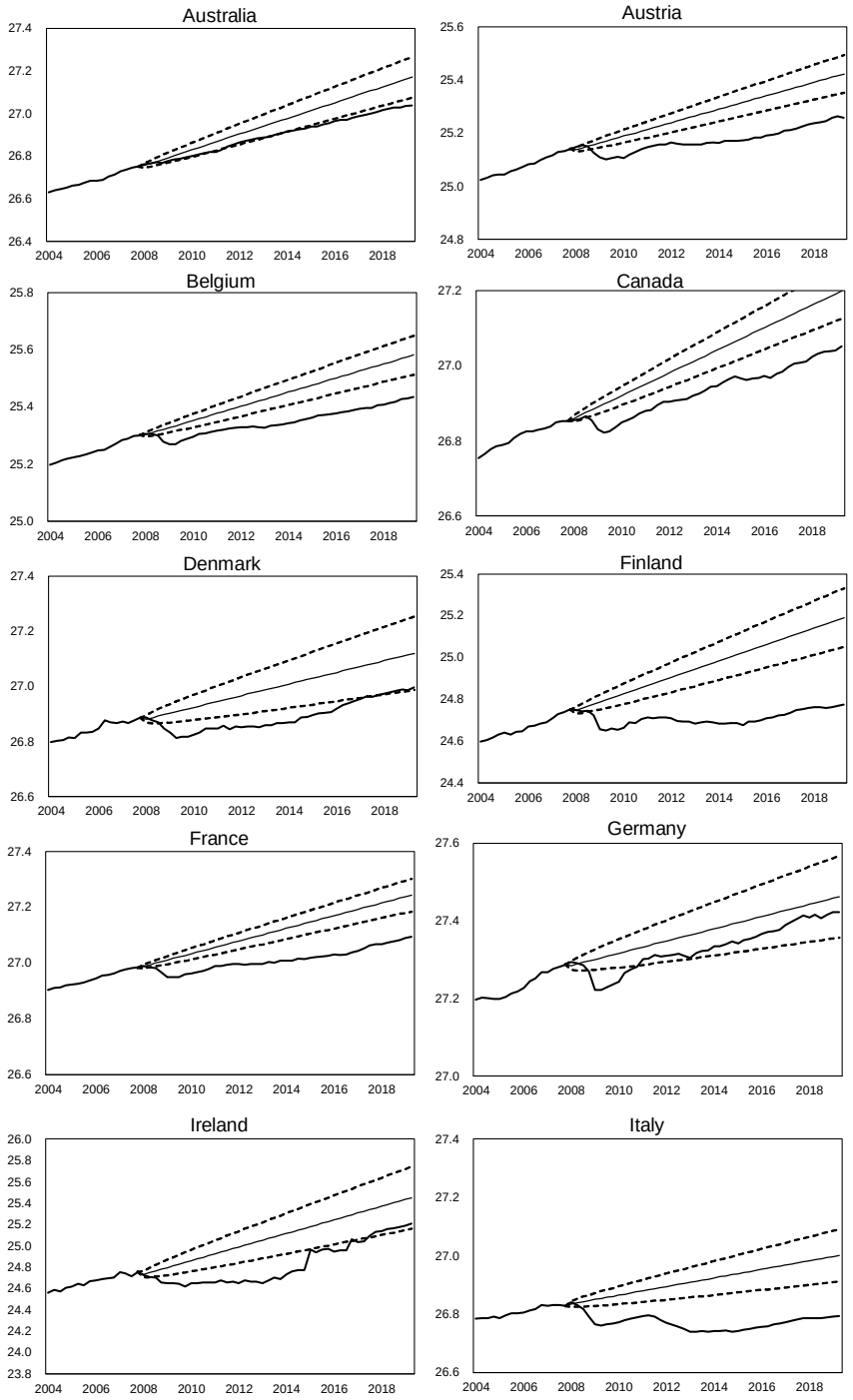

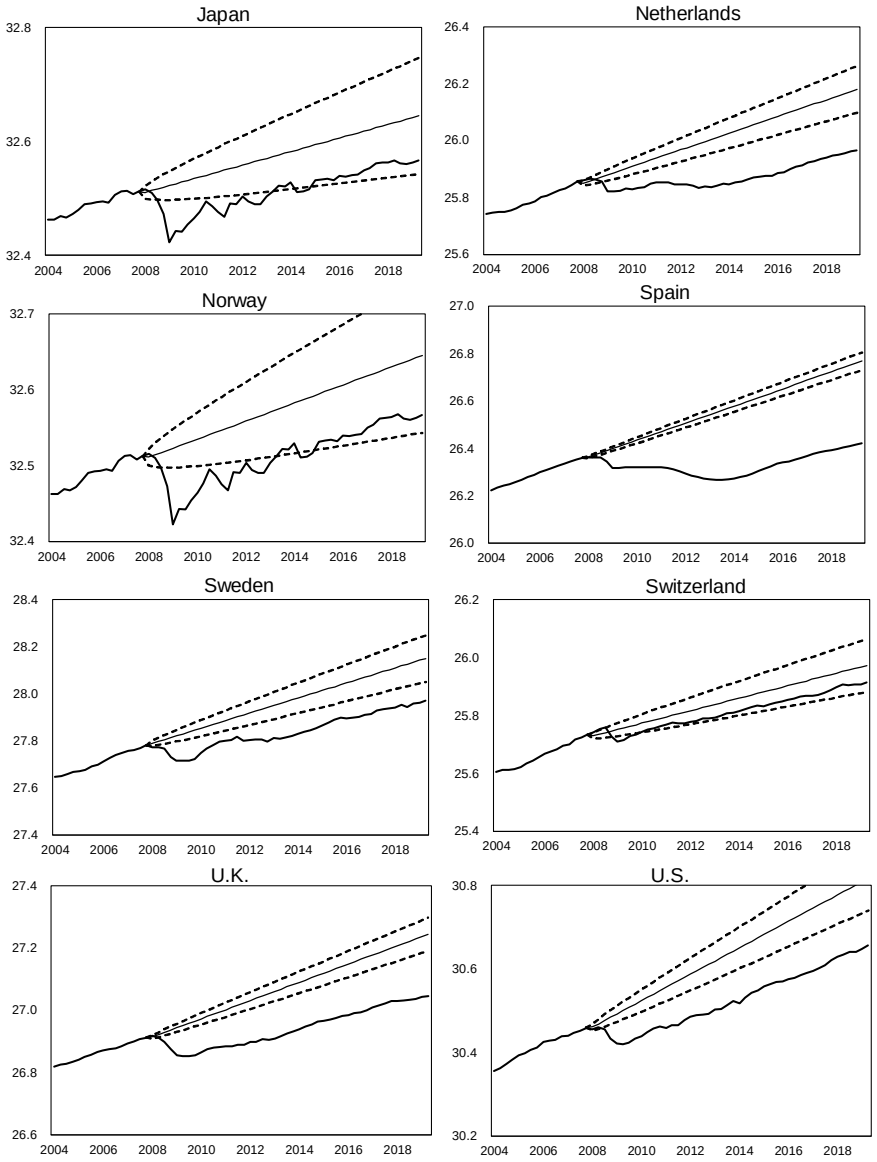
Japan
32.8
32.6
32.4
2004 2006 2008 2010 2012 2014 2016 2018
Netherlands
26.4
26.2
26.0
25.8
25.6
2004 2006 2008 2010 2012 2014 2016 2018
Norway
32.7
32.6
32.5
32.4
2004 2006 2008 2010 2012 2014 2016 2018
Spain
27.0
26.8
26.6
26.4
26.2
26.0
2004 2006 2008 2010 2012 2014 2016 2018
Sweden
28.4
28.2
28.0
27.8
27.6
27.4
2004 2006 2008 2010 2012 2014 2016 2018
Switzerland
26.2
26.0
25.8
25.6
25.4
2004 2006 2008 2010 2012 2014 2016 2018
U.K.
27.4
27.2
27.0
26.8
26.6
2004 2006 2008 2010 2012 2014 2016 2018
U.S.
30.8
30.6
30.4
30.2
2004 2006 2008 2010 2012 2014 2016 2018

**Figure 5. Counterfactual Forecast Interval after COVID-19**

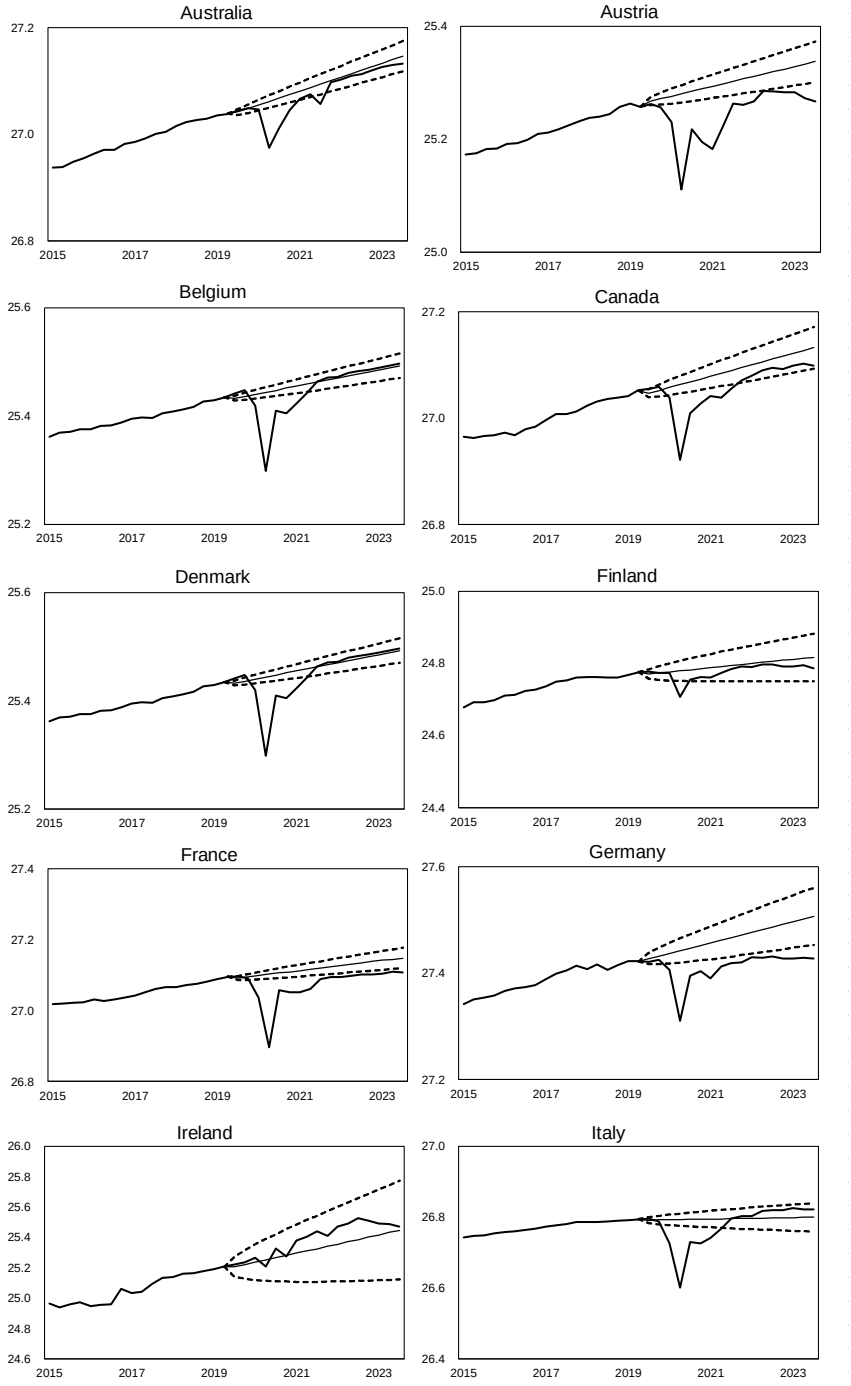

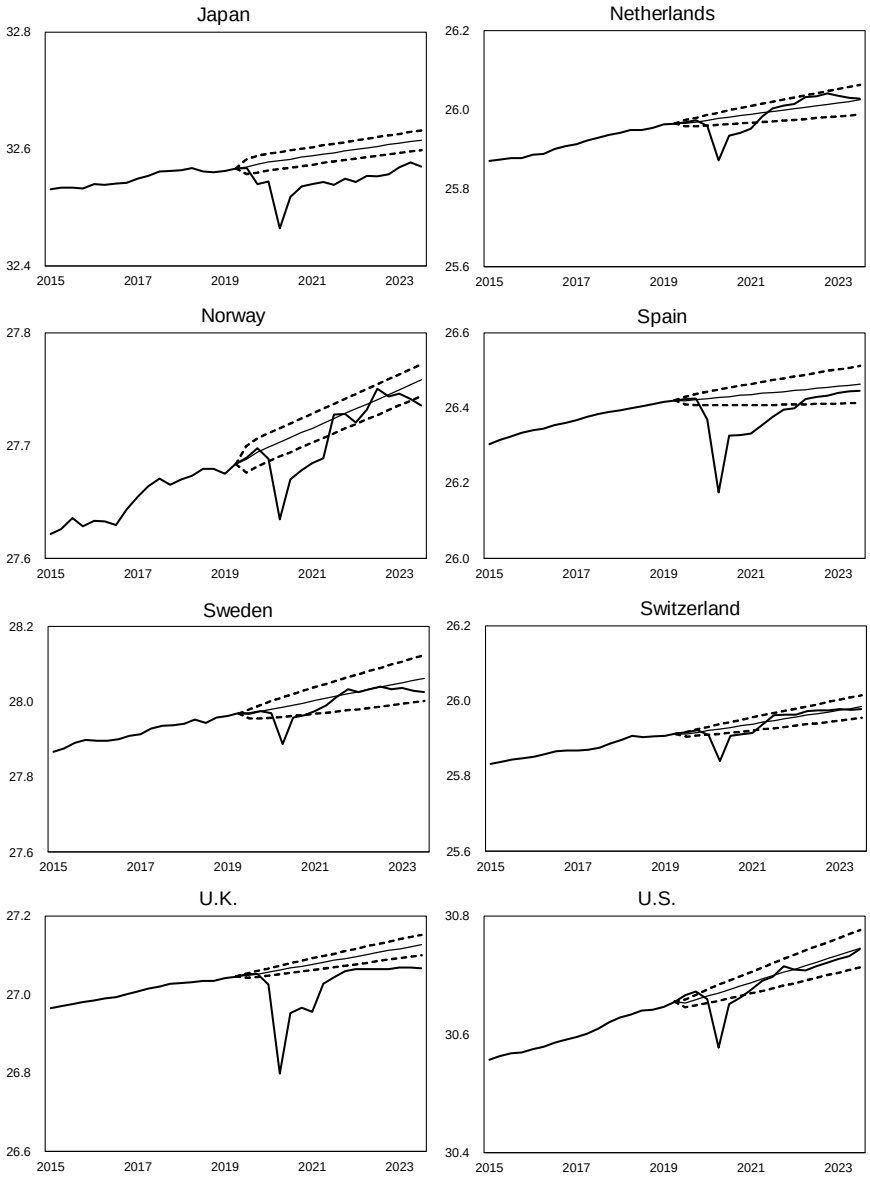
Japan
32.8
32.6
32.4
2015
2017
2019
2021
2023
Netherlands
26.2
26.0
25.8
25.6
Norway
27.8
27.7
27.6
Spain
26.6
26.4
26.2
26.0
Sweden
28.2
28.0
27.8
27.6
Switzerland
26.2
26.0
25.8
25.6
U.K.
27.2
27.0
26.8
26.6
U.S.
30.8
30.6
30.4

**Table 3. Absorption ($s^*$) and Recovery ($RQ_H$) Statistics**

| | GFC | | COVID-19 | |
|---|---|---|---|---|
| | absorption | recovery | absorption | recovery |
| Australia | -2.19 | 0.12 | -11.34 | 0.74 |
| Austria | -5.78 | 0.20 | -16.68 | 0.68 |
| Belgium | -5.75 | 0.25 | -22.97 | 0.85 |
| Canada | -6.29 | 0.30 | -12.97 | 0.75 |
| Denmark | -4.13 | 0.23 | -6.23 | 0.94 |
| Finland | -6.03 | 0.13 | -3.95 | 0.75 |
| France | -6.81 | 0.18 | -25.17 | 0.78 |
| Germany | -4.74 | 0.53 | -8.80 | 0.63 |
| Ireland | -3.93 | 0.02 | -0.59 | 1.70 |
| Italy | -6.05 | 0.18 | -16.45 | 0.87 |
| Japan | -6.03 | 0.53 | -13.23 | 0.50 |
| Netherlands | -7.75 | 0.08 | -9.95 | 0.86 |
| Norway | -2.76 | 0.16 | -9.30 | 0.69 |
| Spain | -21.01 | 0.08 | -17.79 | 0.75 |
| Sweden | -6.03 | 0.30 | -5.89 | 0.79 |
| Switzerland | -3.11 | 0.44 | -10.28 | 0.86 |
| U.K. | -10.88 | 0.15 | -35.94 | 0.75 |
| U.S. | -6.32 | 0.18 | -10.82 | 0.83 |
| AVE | -6.31 | 0.23 | -13.24 | 0.82 |
| SD | 4.14 | 0.15 | 8.43 | 0.24 |

## Figure 6. Standardized Statistics

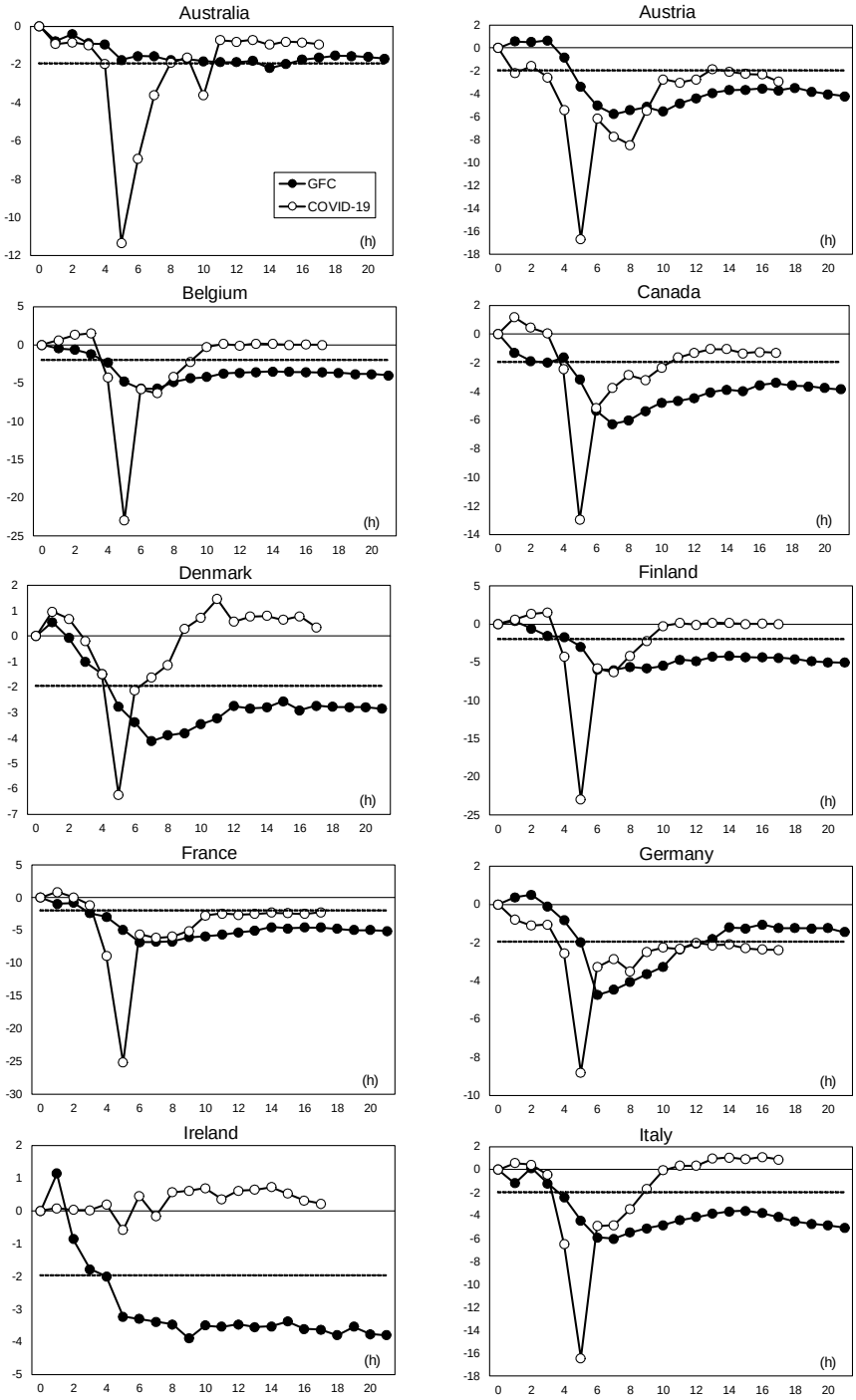

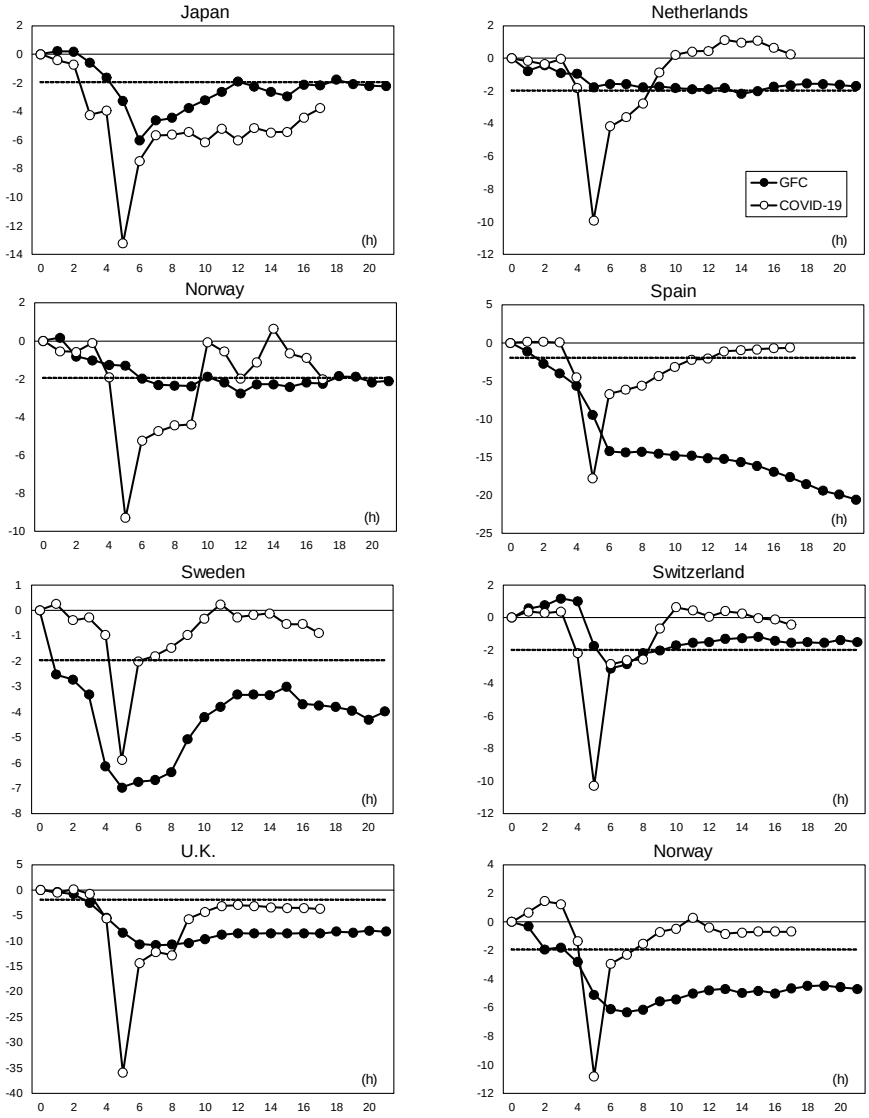
Japan
Netherlands
Norway
Spain
Sweden
Switzerland
U.K.
Norway
GFC
COVID-19
(h)

**Figure 7. Associations of Economic Resilience with Potential Determinants**

**A. Government Debt**

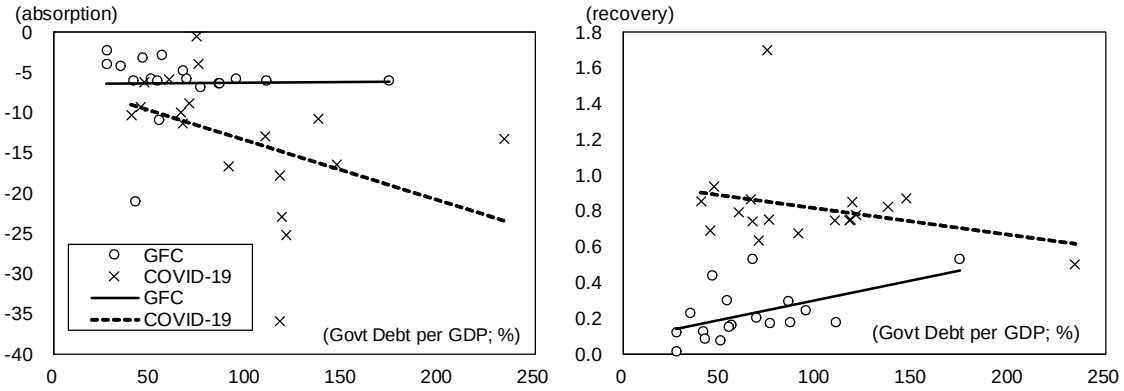


**B. Financial Leverage**

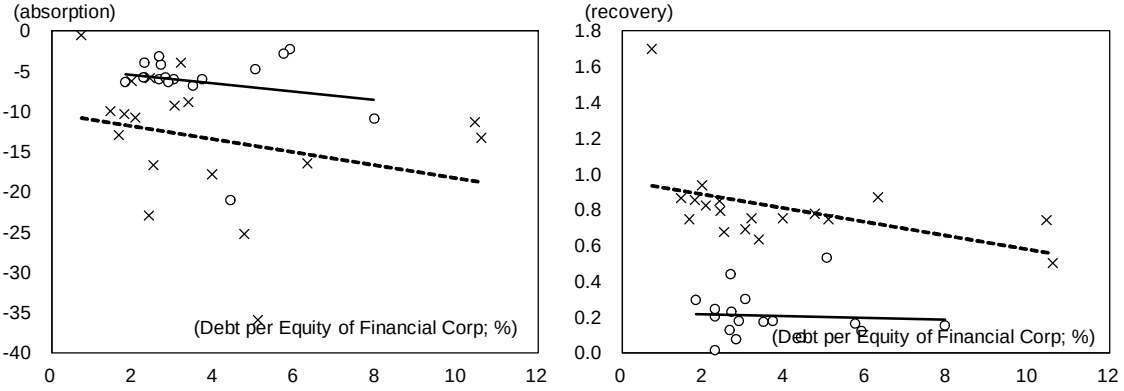


**C. R&D Spending**

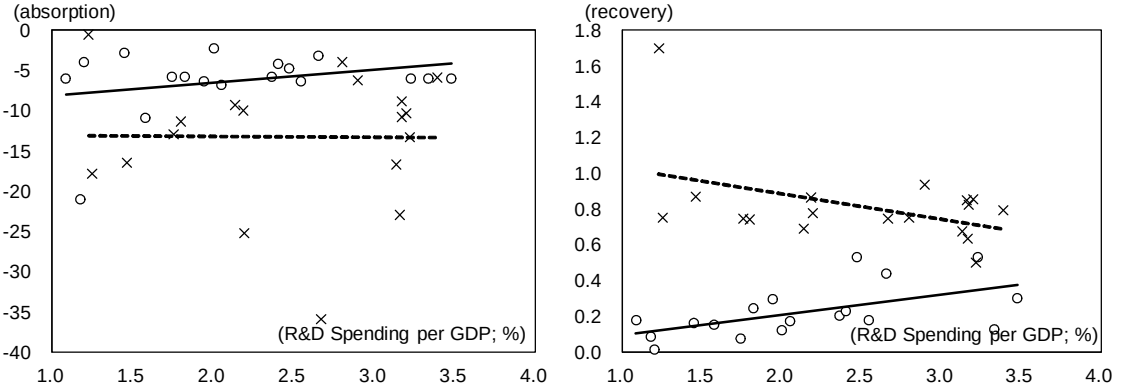

**D. Labor Market Regulation**

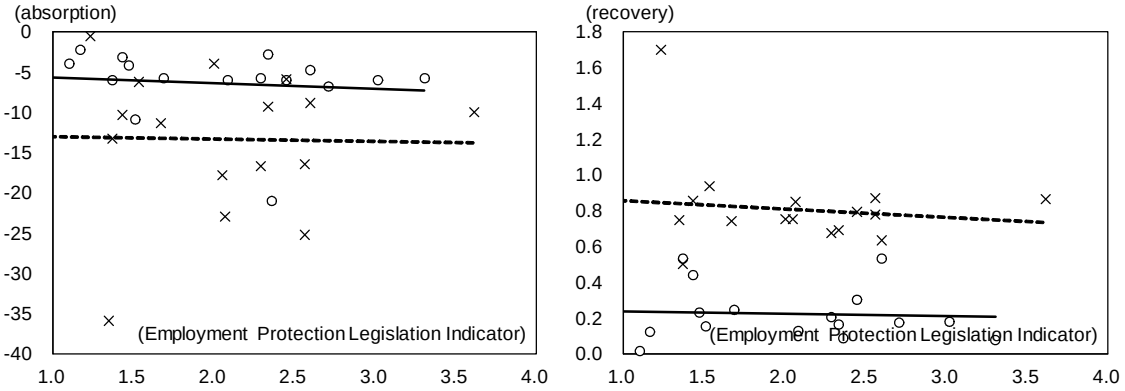


**E. Trade Openess**

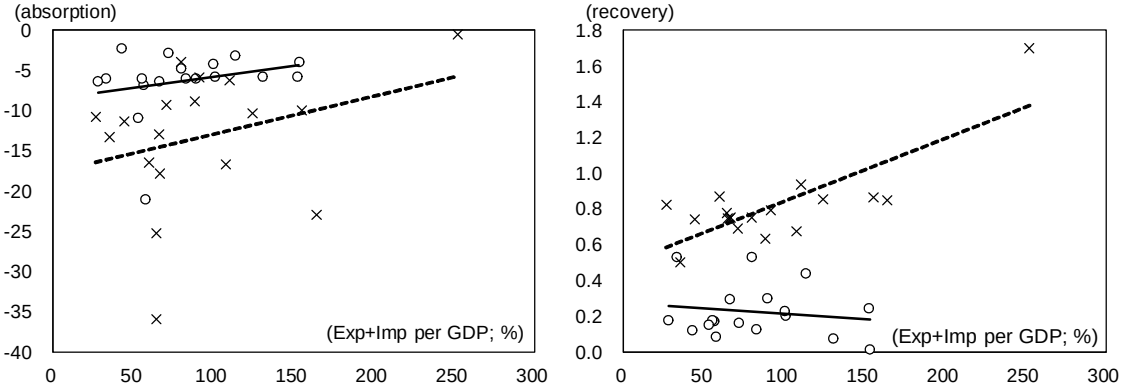


**F. Inequality**

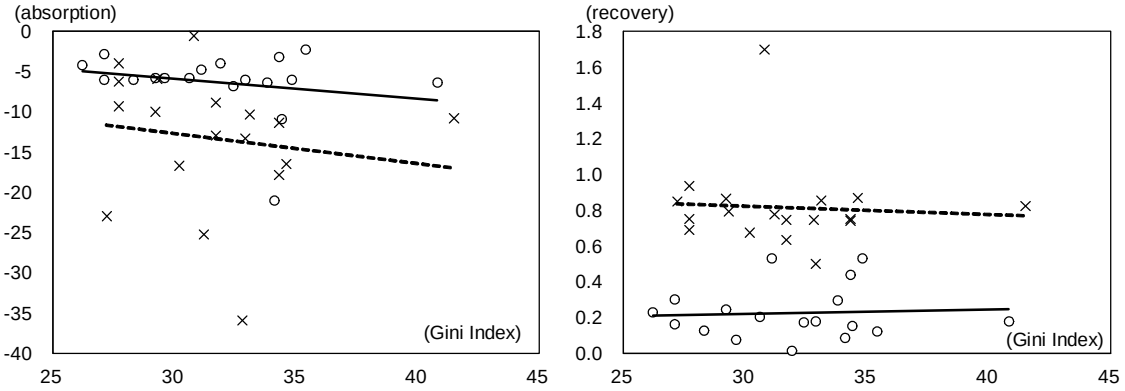

**Table A1-a. Coverage Rate and Average Length of Forecasting Intervals ($T = 50$)**

| | Coverage rate | | | | Average length | | | |
|---|---|---|---|---|---|---|---|---|
| | *h=1* | *h=10* | *h=25* | *h=50* | *h=1* | *h=10* | *h=25* | *h=50* |
| *ρ=0.0* | | | | | | | | |
| TS-FGLS | 0.90 | 0.89 | 0.90 | 0.90 | 3.40 | 3.48 | 3.67 | 4.08 |
| TS-OLS | 0.90 | 0.89 | 0.90 | 0.90 | 3.44 | 3.52 | 3.71 | 4.14 |
| PT-FGLS | 0.90 | 0.89 | 0.90 | 0.90 | 3.40 | 3.48 | 3.67 | 4.08 |
| PT-OLS | 0.90 | 0.89 | 0.90 | 0.90 | 3.44 | 3.52 | 3.71 | 4.14 |
| *ρ=0.5* | | | | | | | | |
| TS-FGLS | 0.88 | 0.87 | 0.85 | 0.85 | 3.40 | 4.19 | 4.64 | 5.60 |
| TS-OLS | 0.89 | 0.87 | 0.86 | 0.86 | 3.44 | 4.30 | 4.82 | 5.91 |
| PT-FGLS | 0.88 | 0.88 | 0.86 | 0.86 | 3.42 | 5.01 | 6.45 | 8.81 |
| PT-OLS | 0.88 | 0.88 | 0.87 | 0.87 | 3.46 | 5.09 | 6.58 | 9.03 |
| *ρ=0.8* | | | | | | | | |
| TS-FGLS | 0.88 | 0.80 | 0.79 | 0.77 | 3.39 | 5.86 | 6.95 | 8.90 |
| TS-OLS | 0.89 | 0.81 | 0.80 | 0.79 | 3.43 | 6.27 | 7.84 | 10.62 |
| PT-FGLS | 0.89 | 0.92 | 0.93 | 0.92 | 3.46 | 10.49 | 18.01 | 29.06 |
| PT-OLS | 0.89 | 0.92 | 0.92 | 0.92 | 3.46 | 10.51 | 18.05 | 29.14 |
| *ρ=0.9* | | | | | | | | |
| TS-FGLS | 0.88 | 0.74 | 0.69 | 0.67 | 3.37 | 6.93 | 8.66 | 11.38 |
| TS-OLS | 0.88 | 0.75 | 0.72 | 0.70 | 3.41 | 7.64 | 10.66 | 15.80 |
| PT-FGLS | 0.89 | 0.91 | 0.94 | 0.95 | 3.40 | 11.17 | 19.57 | 31.87 |
| PT-OLS | 0.89 | 0.91 | 0.94 | 0.95 | 3.40 | 11.18 | 19.59 | 31.90 |
| *ρ=0.95* | | | | | | | | |
| TS-FGLS | 0.88 | 0.71 | 0.62 | 0.58 | 3.34 | 7.47 | 9.66 | 12.86 |
| TS-OLS | 0.88 | 0.73 | 0.66 | 0.64 | 3.38 | 8.40 | 12.77 | 20.78 |
| PT-FGLS | 0.89 | 0.90 | 0.92 | 0.94 | 3.35 | 11.15 | 19.58 | 31.93 |
| PT-OLS | 0.89 | 0.90 | 0.92 | 0.94 | 3.35 | 11.15 | 19.59 | 31.95 |
| *ρ=1.0* | | | | | | | | |
| TS-OLS | 0.88 | 0.67 | 0.56 | 0.47 | 3.29 | 7.71 | 10.22 | 13.75 |
| TS-FGLS | 0.88 | 0.70 | 0.62 | 0.56 | 3.33 | 8.86 | 14.48 | 25.67 |
| PT-FGLS | 0.89 | 0.86 | 0.86 | 0.85 | 3.29 | 10.99 | 19.33 | 31.52 |
| PT-OLS | 0.89 | 0.86 | 0.86 | 0.86 | 3.29 | 10.99 | 19.33 | 31.54 |

**Table A1-b. Coverage Rate and Average Length of Forecasting Intervals ($T = 100$)**

| | Coverage rate | | | | Average length | | | |
|---|---|---|---|---|---|---|---|---|
| | *h=1* | *h=10* | *h=25* | *h=50* | *h=1* | *h=10* | *h=25* | *h=50* |
| *ρ=0.0* | | | | | | | | |
| TS-FGLS | 0.89 | 0.91 | 0.90 | 0.89 | 3.35 | 3.36 | 3.40 | 3.48 |
| TS-OLS | 0.90 | 0.91 | 0.90 | 0.90 | 3.36 | 3.38 | 3.42 | 3.50 |
| PT-FGLS | 0.89 | 0.91 | 0.90 | 0.89 | 3.35 | 3.36 | 3.40 | 3.48 |
| PT-OLS | 0.90 | 0.91 | 0.90 | 0.90 | 3.36 | 3.38 | 3.42 | 3.50 |
| *ρ=0.5* | | | | | | | | |
| TS-FGLS | 0.89 | 0.89 | 0.89 | 0.88 | 3.34 | 3.96 | 4.08 | 4.31 |
| TS-OLS | 0.89 | 0.89 | 0.89 | 0.88 | 3.36 | 4.00 | 4.12 | 4.37 |
| PT-FGLS | 0.89 | 0.89 | 0.89 | 0.88 | 3.34 | 3.96 | 4.08 | 4.31 |
| PT-OLS | 0.89 | 0.89 | 0.89 | 0.88 | 3.36 | 4.00 | 4.12 | 4.37 |
| *ρ=0.8* | | | | | | | | |
| TS-FGLS | 0.89 | 0.84 | 0.85 | 0.84 | 3.34 | 5.70 | 6.14 | 6.80 |
| TS-OLS | 0.89 | 0.85 | 0.85 | 0.85 | 3.36 | 5.85 | 6.39 | 7.20 |
| PT-FGLS | 0.88 | 0.87 | 0.87 | 0.87 | 3.37 | 7.35 | 10.24 | 14.22 |
| PT-OLS | 0.88 | 0.87 | 0.87 | 0.87 | 3.38 | 7.42 | 10.34 | 14.38 |
| *ρ=0.9* | | | | | | | | |
| TS-FGLS | 0.90 | 0.82 | 0.79 | 0.77 | 3.34 | 7.13 | 8.27 | 9.50 |
| TS-OLS | 0.90 | 0.82 | 0.81 | 0.79 | 3.36 | 7.39 | 8.95 | 10.77 |
| PT-FGLS | 0.90 | 0.91 | 0.92 | 0.93 | 3.37 | 10.11 | 16.40 | 24.91 |
| PT-OLS | 0.90 | 0.91 | 0.92 | 0.93 | 3.37 | 10.13 | 16.43 | 24.97 |
| *ρ=0.95* | | | | | | | | |
| TS-FGLS | 0.89 | 0.79 | 0.73 | 0.68 | 3.33 | 8.06 | 10.03 | 11.96 |
| TS-OLS | 0.89 | 0.80 | 0.75 | 0.70 | 3.35 | 8.43 | 11.25 | 14.64 |
| PT-FGLS | 0.90 | 0.90 | 0.92 | 0.94 | 3.34 | 10.61 | 17.62 | 27.09 |
| PT-OLS | 0.90 | 0.90 | 0.92 | 0.94 | 3.34 | 10.62 | 17.63 | 27.11 |
| *ρ=1.0* | | | | | | | | |
| TS-OLS | 0.89 | 0.76 | 0.65 | 0.55 | 3.29 | 8.71 | 11.62 | 14.48 |
| TS-FGLS | 0.89 | 0.77 | 0.68 | 0.60 | 3.31 | 9.21 | 13.71 | 20.27 |
| PT-FGLS | 0.90 | 0.88 | 0.87 | 0.86 | 3.29 | 10.60 | 17.69 | 27.29 |
| PT-OLS | 0.90 | 0.88 | 0.87 | 0.86 | 3.29 | 10.60 | 17.69 | 27.28 |